

## Study Of Tribological Features Of AA6082 Material Coated With Micro Arc Oxidation (MAO) Method At Different Lubricating Conditions

Yusuf Başoğul<sup>a,\*</sup>, Ertuğrul Durak<sup>b</sup>, Uğur Malayoğlu<sup>c</sup>

<sup>a</sup>,Adiyaman University, Department of Mechanical Engineering, Adiyaman, Turkey

<sup>b</sup> Süleyman Demirel University, Department of Mechanical Engineering, Isparta, Turkey

<sup>c</sup> Dokuz Eylül University, Department of Metallurgical and Materials Engineering, Izmir, Turkey

\*Corresponding Author: Yusuf Başoğul

**ABSTRACT:** In this study, the tribological features of AA6082 test samples that were coated with Micro Arc Oxidation (MAO) method and that are not coated at 0,146, 0,292, 0,438 m/sliding velocities and 50, 100, 150 N loads, 500 m sliding distances and different lubricating conditions were studied with Pin on Disc Wear Test Rig (PDWTR) and Reciprocating Test Rig (RTR). Within the scope of the study; coating thickness measurements, friction coefficient ( $\mu$ ), wear ratio ( $W$ ) and wear amount, surface roughness measurements, macro image reviews of the specimen samples, scanned electron microscope (SEM) of the samples, energy distribution x ray spectrum (EDX), X-ray diffraction (XRD) and atomic force microscope (AFM) studies were done. While friction coefficients of MAO coated samples were detected generally higher compared to uncoated samples both at continuous lubricant feeding (CLFCL) conditions and intermittent lubricant feeding lubricating condition (ILFLC), their wear ratios were detected lower.

**KEY WORDS:** AA6082, Micro Ark Oxidation (MAO), friction coefficient, wear, lubrication

Date of Submission: 31-07-2018

Date of acceptance: 15-08-2018

### I. INTRODUCTION

Automotive manufacturers confront challenges to enhance the performance of vehicle by reducing vehicle weight, improving fuel economy, reducing emissions, and improving vehicle safety. It is urgent to develop materials with low density and high strength that can be used in body structures or joints in automotive production [1]. Aluminum alloys, which are strategically and structurally important materials due to their high specific strength, suffer from moderately poor tribological properties. Surface-modified wear-resistant aluminum alloys have been increasingly finding numerous applications in today's industries [2]. In so many industry branches, so much effort is made with the aim of meeting the appropriate new technology product material requests for the working conditions that has become more complicated day by day. Within this direction, the studies concerning to developing current features of the materials as bound to the desired conditions have been carried out. In the recent years, it has been tended towards gaining more appropriate and commonly used materials through combining the metals that are qualified as formability and generally satiated materials as plastic and the ceramics whose friction and corrosion resistance is relatively higher. One of these applications is to form a ceramic layer on surfaces of metallic materials [3]. Ceramic coatings are applied with the aim of increasing resistance of the materials to the heat, corrosion and wear. While desired features may be achieved thanks to these ceramic coatings whose hardness is higher compared to the metals, other features such as easy formability and toughness may be protected. Therefore ceramic coatings allow for that superior features of ceramic and metal materials may be combined and used together [3,4] These are the factors that optimize the coating technology: operating temperature, conformity of substrate material and coating, coating composition, porosity amount, life of the coating, material losses and adhesion. One of the most advantageous sides of coating technology is that it provides long coating life expected from a coated system [5] MAO, also known as Plasma Electrolytic Oxidation (PEO), Spark Anodizing and Microplasma Oxidation, is a processing technique in which the surfaces of metals such as aluminum, magnesium and titanium are converted into oxide

coatings. In general, the MAO coatings deposited on Al alloys predominantly contain  $\alpha$ -Al<sub>2</sub>O<sub>3</sub> and  $\gamma$ -Al<sub>2</sub>O<sub>3</sub> phases [6]

These coatings can range from tens to hundreds of microns in thickness, depending on the power supply, substrate and electrolyte used. The process is known to involve large numbers of short-lived sparks (electrical discharges), caused by localized electrical breakdown of the growing coating. These discharges clearly play an important role in the coating growth mechanism. They leave characteristic "craters" on the free surface of the growing coating [7].

MAO coatings attract attention with its ultimately high hardness value, wear resistance, corrosion resistance and its strong adhesion with the substrate material. It competes especially with plasma spray and EB-PVD (electron beam physical stem deposition) coatings due to high hardness and friction resistances. In terms of protection from corrosion and adhesion feature, they compete with anode coatings. MAO process is carried out on light metals (Al, Mg, Ti, Zr, Hf, Ta, etc.) and alloys of these at wide range and it is known that the coating feature is bound on the substrate material [3].

So many parameter of the process may be optimized for each remarkable alloy and applications. These applications include electrolyte compositions that are formed through changing the modified components included in the coating. These effects affects growth rate of the coating and efficiency of obtained coating features to the process. MAO process is a very fast and at the same time environment friend procedure. The procedure before the coating process is very effortless and the only procedure that is required is the procedure concerning to cleaning of the substrate material and purifying from the lubricant. The process is ultimately safe and dilute and nontoxic electrolyte is needed. While it is a costly production method in term of economy, the process is resistant to the competition due to it has similar cost with the commercial anodizing when arrangement of the electrolyte components are taken into consideration [8] In recent years, investigations on the phase composition, mechanical and tribological properties of MAO coatings on Ti, Mg, Al and their alloys were done by many researchers. However, the tribological performances of MAO coatings are not only affected by the intrinsic properties of MAO coatings, but also affected by many extrinsic factors, such as load, sliding speed, counterpart materials, lubrication conditions, temperature and humidity etc [9].

Although several studies have been carried out, the complete tribological characteristics of MAO coatings exposed to different kinds of lubrication have not been studied. In this study, tribological features of AA6082 test samples that were coated with MAO and that were not coated such as friction and wear resistance were reviewed at different velocities and loads and 500 m sliding distance and different lubricating conditions with PDWTR and RTR apparatus [11] In this study; it was aimed to make contribution to the boundaryed literature with continuous lubricant feeding (CLFLC) and intermittent lubricant feeding (ILFLC) lubricating conditions (approximately 2-3 drops lubricant deliver was done per 15 minutes) of MAO coated materials.

## II. EXPERIMENTAL STUDY

### 2.1. Material of the Specimen and Its Preparation

The data concerning to coating procedure, friction and wear experiment apparatus and experimental conditions in this study were summarized in Table 1. The system that was used in MAO coating procedure and the coating formation at AA6082 samples during Micro Arc Oxidation procedure is given in Figure 1.

**Table 1. Data of the experimental study**

Substrata material	AA 6082
Pre-preparation procedures	After the samples were rubbed down with SiC at 360-1200 grid and cleaned with alcohol and acetone in the ultrasonic bath, they were rinsed with pure water.
Diameter and length of the sample (mm)	Ø 10, 30
Electrolyte	1 g/l KOH solid and 3 g/l Na <sub>2</sub> SiO <sub>3</sub> aqueous solution
PH	10,677
Density of the current ( A/cm <sup>2</sup> )	0,2
Voltage (V)	220
Type and power of the power unit	DC - 30kW
Procedure temperature	20°C
Period of the procedure (minute)	30
Disc Material and the opposite material at the reciprocating test, its hardness (HV), Surface Roughness (Ra, µm)	AISI 8620, 670 HV 50/10, 0,153
Material and Chemical Composition of Test Sample (%)	AA6082, Si (% 0.85), Fe (%0.50), Cu (%0,09), Mn (%0,35), Mg (%0,98), Zn (%0,07), Cr (0,01), Others (%0,319), Al(%96,831)
Load (N)	50 – 100 - 150
Sliding velocity (m/s)	0,146 - 0,292 – 0,438
Sliding Distance (m)	5000
Density of the lubricant 15 °C (g/cm <sup>3</sup> )	0,8867
Viscosity of the lubricant @ 40°C (cSt)	179,88

Viscosity of the lubricant @ 100°C (cSt)	19,37
Viscosity Index of the lubricant (VI)	123
Experiment Lubricant Temperature(°C)	40

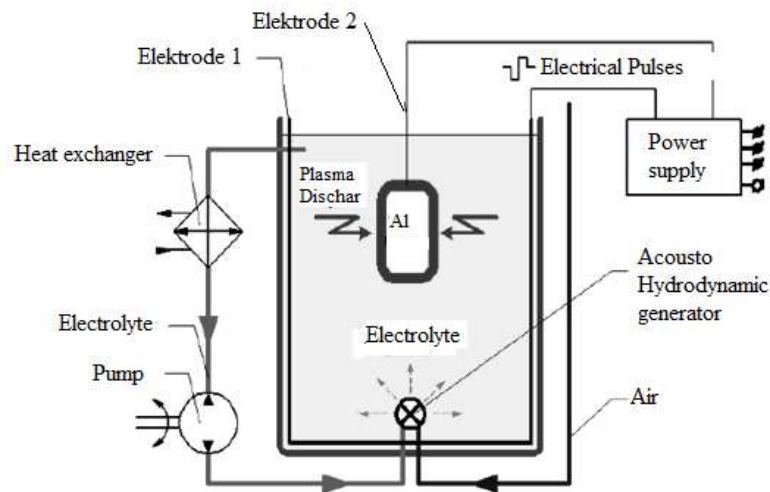


Figure 1. Micro Arc Oxidation Circuit Scheme [11]

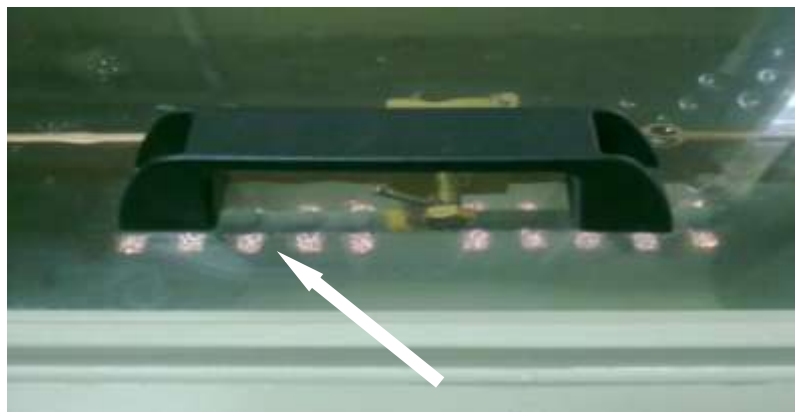


Figure2. The coating formation at AA6082 samples during Micro Arc Oxidation procedure

## 2.2. Structural Examinations

For the phase assignment of the coatings, Shimadzu branded device that was able to make phase assignment with diffraction method of X-rays. The phase assignment was done by making a 2 degree/minute fast scanning up to  $10^{\circ}$ - $90^{\circ}$  with the x-rays detector and collecting x-rays beams that were exposed to diffraction. Copper  $K\alpha$  X-ray at  $1,544 \text{ \AA}$  wavelength was used in x-rays analysis. Also screening was done with SEM device (LEO 1430 VP model) and x-rays (EDX- Energy Dispersive X-ray Spectroscopy) at the detection of friction statuses on the surfaces of MAO coated and uncoated samples by MAO method.

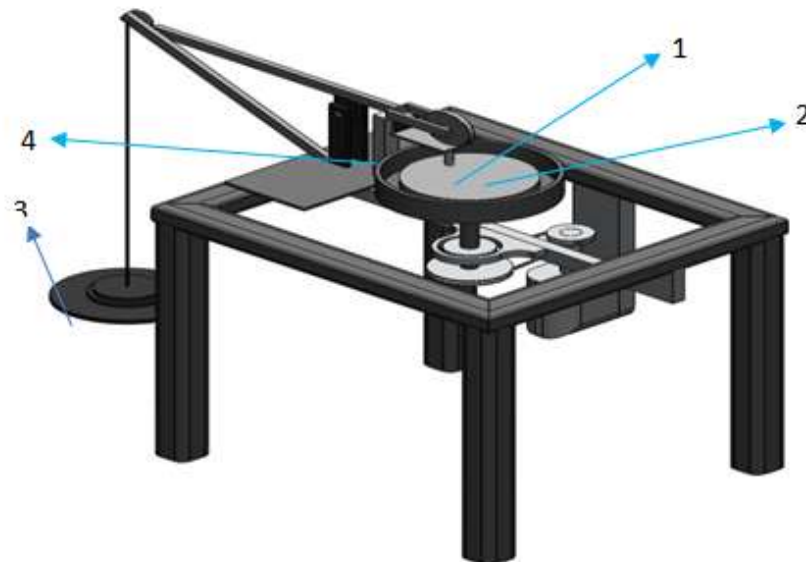
## 2.3. Mechanical Tests

### 2.3.1. Hardness Measurement of the Coating

To be able to make hardness measurements of coating surface regions, average roughness ( $R_a$ ) of coating surface were polished as  $R_a < 0,5 \mu\text{m}$ . To be able to measure the hardness at inter section, sections of coated material were taken to bakelite and then rubbed down and they were exposed to polishing procedure until they reached a lower surface roughness values. After hardness measurements at equal distances from coating inter surface along the coating thickness were carried out, the arithmetic mean was taken and then hardness values were detected. 70 g load was applied in the experiments within 10 sections.

### 2.3.2. Friction and Wear Tests

First group experiments were carried out on PDWTR (Figure 2). The material of the disc that was used in this test rig was chosen as alloy steel (AISI 8620) and its surface was hardened after it was processed with machining. Then the disc surface was grinded. All experiments were done by using mineral base lubricant at the sliding velocities, loads and sliding distance were summarized in Table 1. The average coefficient of friction was calculated from the change of the friction coefficient during the test for each test.



1-Pin 2- Disc 3- Load 4- Loadcell

Figure 0.1 Test Apparatus of Pin Disc Wear [12]

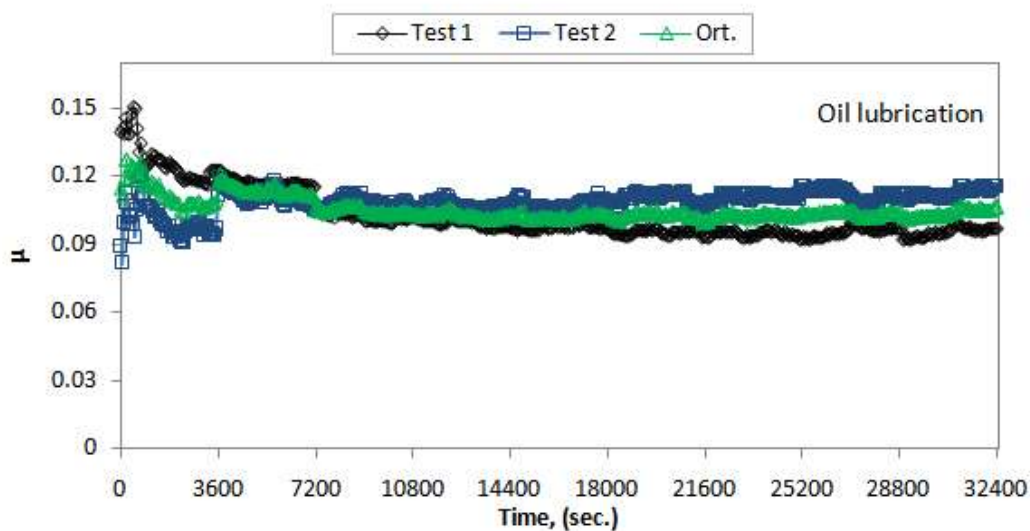
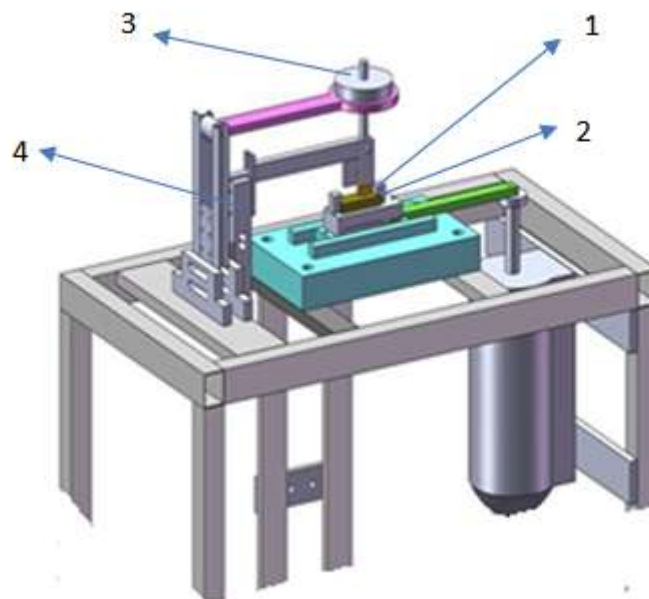


Figure 4.  $\mu$  change of AA 6082 uncoated sample based on the sample time (CLFLC condition, 50N, 0,146 m/s,)

The second group experiments were done at RTR. It was done over a test apparatus that is operated pursuant to measurement principle of the friction force between the opposite contact material (AISI 8620) being same to the disc material used on PDWTR counter attached a plate having a reciprocating (linear, offset) with special lugs and fixed Pin test sample (Figure 2).



1-Pin 2- Plate 3- Load 4- Loadcell

Figure 5. Friction Test Apparatus of Reciprocating[13]

As an example to submission of gained test results in the article, measurements of friction coefficients of uncoated and MAO coated Pin samples at 150 N load and 0,146 m/s sliding velocity under ILFLC lubricating conditions are given.  $\mu$  at going (forward) movement in the positive (+ symbol) and coming (backward) movement in the negative (- symbol) region is shown.

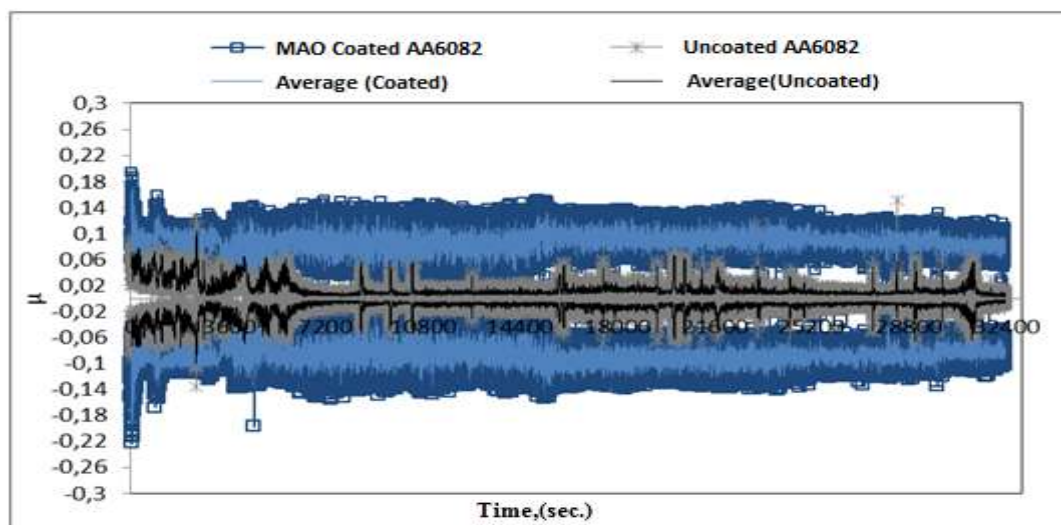


Figure 6.  $\mu$  change of AA6082 sample at  $F=150$  N and 0,146 m/s sliding velocity in the sample experiments along the experiment

### III. RESULTS AND DISCUSSION

#### 3.1. Results of the Micro Structure

The coatings were produced with the aim of obtaining a MAO coating with  $Al_2O_3$  phase in accordance with the conditions stated on AA6082 alloy. SEM images of MAO coated AA6082 alloy is given Figure 3. The produced coatings were shown in the uniform thickness. The structural studies that were done on aluminum alloys with MAO method showed that generally a porous external region and an inner region that was deemed more frequent was formed in the coatings. [14-16]. And sometimes a fine intermediate transverse region was formed under the dense layer[17]. It was clearly seen in this study that porous external region was formed as stated in the literature and at the same time, a sense and a fine intermediate surface region was more frequently formed under it.

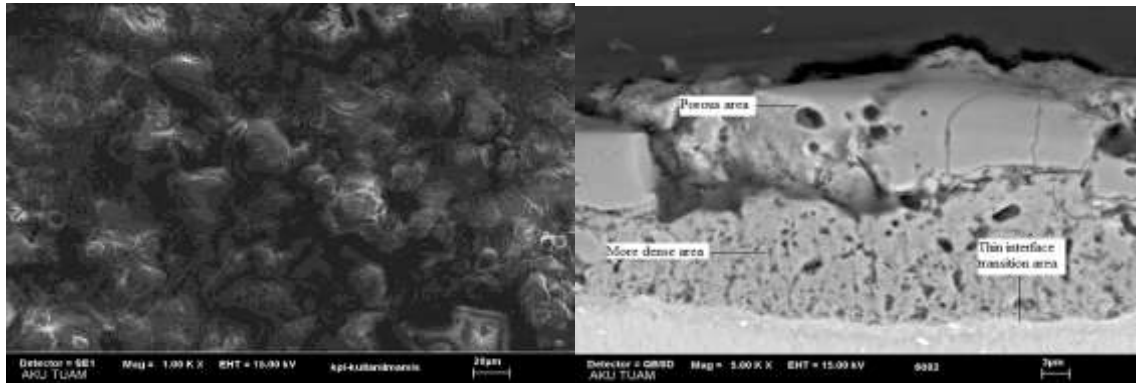


Figure 7. SEM images of micro surface and micro structure of MAO coating done over AA6082 alloy

### 3.2. X-Ray Analysis (XRD) Studies

MAO procedure that was done depending on the current, electrolyte and period determined before the experiments (Table 1.) was carried out through making XRD analysis for the phase detection available in AA6082 with elemental composition of the coating formed over the aluminum substrate material. The phase composition of the coating that was one of the important factors that affected mechanical and tribological features of coating surface is given at Figure 4 and it was formed from  $\gamma$ - $\text{Al}_2\text{O}_3$  and Al phases [18,20]. The other phases (Mullite and  $\alpha$ - $\text{Al}_2\text{O}_3$ ) may be formed when coating process was increased. Mullite and  $\alpha$ - $\text{Al}_2\text{O}_3$  phases were not able to be obtained at test samples due to shortness of coating process (30 minutes) at the coating experiments that were done. The instant potential temperature at MAO coatings reached thousands degree of heat at discharge regions and this situation led to melting of  $\text{Al}_2\text{O}_3$ . When melted oxides were compared with electrolyte, they were solidified and formed  $\gamma$ - $\text{Al}_2\text{O}_3$ ,  $\alpha$ - $\text{Al}_2\text{O}_3$  other phases. A higher cooling ratio at inter section of coating/electrolyte led to the formation of  $\gamma$ - $\text{Al}_2\text{O}_3$ ,  $\alpha$ - $\text{Al}_2\text{O}_3$ . In spite of that,  $\alpha$ - $\text{Al}_2\text{O}_3$  phase at a lower cooling ratio at inner layer was easily formed. Especially,  $\gamma$ - $\text{Al}_2\text{O}_3$  phase at the final stage of MAO process transformed into  $\alpha$ - $\text{Al}_2\text{O}_3$  phase during micro arc discharge. The mullite phase was formed as a result of the reaction of cations that came from sodium silicate electrolyte and melted alumina.<sup>3</sup>

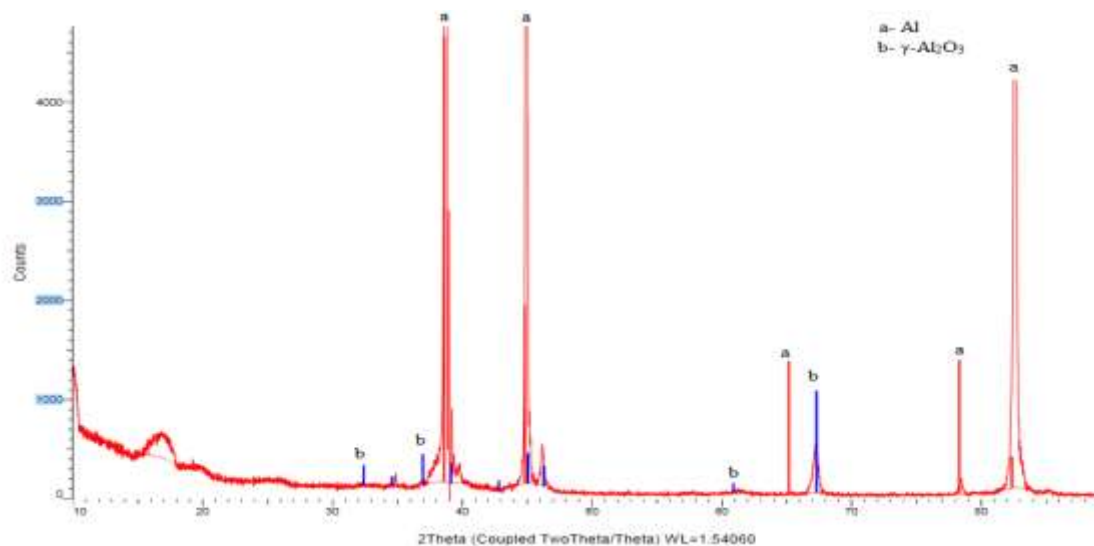
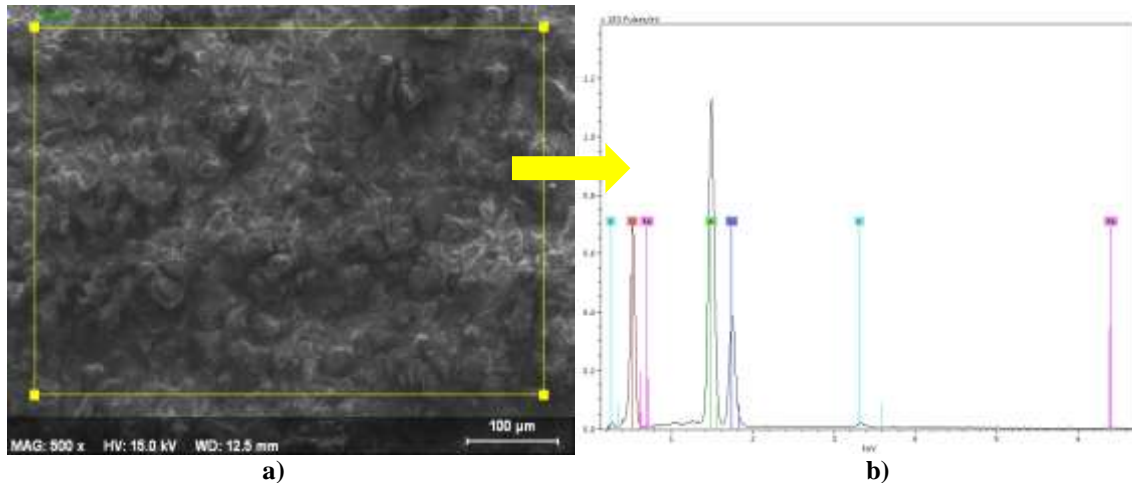


Figure 8. XRD phase structure of AA6082 alloy

### 3.3. Results of EDX Analysis

Elemental composition of coatings and phase ratio were analyzed with energy distribution x-ray spectrometry of LEO 1430 VP SEM device, respectively. The results of EDX analysis that was carried out on the MAO coating formed over AA6082 alloy from the region stated in Figure 5.a is given Figure 5.b. It was understood from EDX analysis that coating was primarily formed from  $\text{Al}_2\text{O}_3$ , alloy elements and electrolyte components were also available in the coating, ferric atom (Figure 5, Table 2) was available within the body of AA6082 alloy. The results of EDX analysis that was carried out in the selected regions of uncoated AA6082 was seen in Figure 6.



**Figure 9. The region selected 500x magnification of AA6082 alloy Al<sub>2</sub>O<sub>3</sub>-based MAO coating and EDX SEM analysis of this region**

It was understood from EDX analysis that coating was primarily formed from Al<sub>2</sub>O<sub>3</sub>, alloy elements and electrolyte components were also available in the coating, ferric atom (Figure 9, Table 2) was available within the body of AA6082 alloy. The results of EDX analysis that was carried out in the selected regions of uncoated AA6082 was seen in Figure 10.

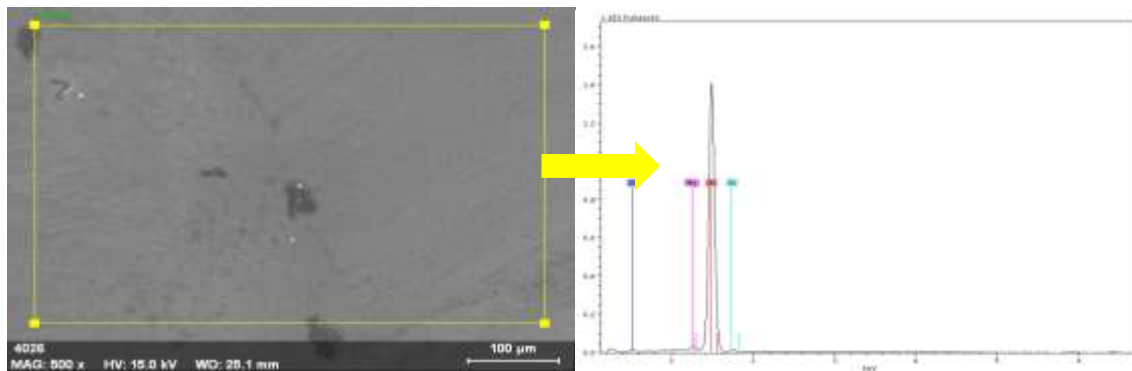


**Figure 10. The region selected 500x magnification of AA6082 alloy and EDX SEM analysis of this region**

As a result of regional EDX analysis that were carried out AA6082 and MAO coatings, average elemental composition (% atomic) was given at Table 2. As seen from Table 2, silicium (Si) and Magnesium (Mg) available inside the aluminum confirmed that atoms were the main alloy elements of AA6082 alloy. It was detected in the analysis that oxygen came to the aluminum from air due to a natural oxidizing.

**Table 2. Average elemental composition of AA6082 and MAO coated alloy as a result of EDX analysis**

Element	O <sub>2</sub>	Al	Si	K	Fe	Mg
% Atomic	MAO Coated					
	72,78	17,78	8,63	0,53	0,26	--
	Uncoated AA6082					
	15,31	81,77	1,47	--	--	1,45

**3.4. Thickness and Surface Roughness Measurement Results of the Coating**

One of the important factors that affect friction and wear resistance of the coatings was coating thickness. The thickness measurements were taken to the bakelite and after the polishing procedure, layer thicknesses at different points were measured by using SEM and arithmetic mean values were measured as approximately 29 μm (± 2 μm). It was seen the thickness measurements were very close to the values of similar studies in the literature. [7,20]

The surface roughness of MAO coated samples before and after the coating as well as whole of uncoated AA6082 alloy and MAO coated samples before and after the friction were measured (Table 4,5,6,7,). R<sub>a</sub> results at MAO coated AA6082 sample was measured as 2,10 - 2,90 μm. These measurements showed that roughness values of coated samples were clearly higher compared to uncoated samples. The reason of this

increase at roughness was related with local fusions inside the arch channels and distribution of melted material.<sup>14</sup> It was seen that roughness measurement results had results that may be deemed as close to the values of similar literature studies[16]. Surface AFM image of sample AA6082 material before and after coating is given at Figure 7.

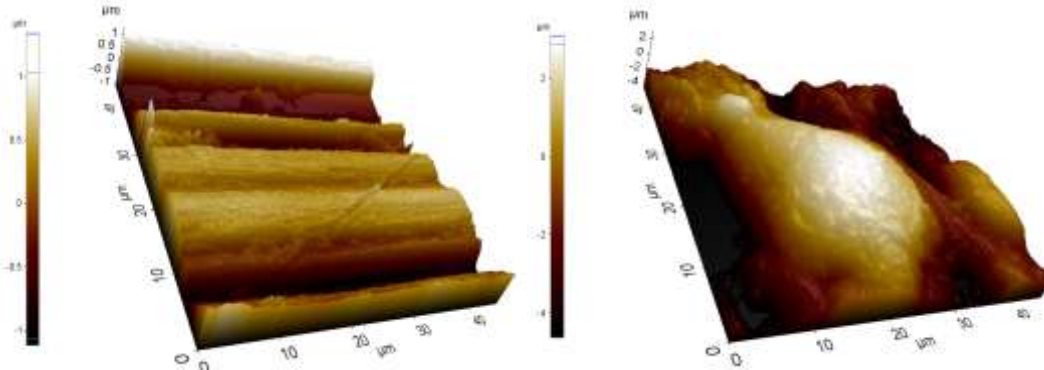


Figure 11. AFM image of AA6082 material a) Before coating b) After coating

**3.5. Hardness Measurements of the Coating**

The hardness value at inter section of MAO coating was detected as 1045 HV 70/10 and the hardness values measured from coating surface was detected as 1095 HV 70/10. The hardness value of substrate material was measured as 102 HV 70/10. It was detected that hardness measurement results were closed to hardness values of coatings stated in the similar studies of the. [15,20,21]

**3.6. The Continuous and Intermittent Lubricant Feeding Tests Results at PDWTR**

At Pin on Disc Friction Test Apparatus,  $\mu$  changes at the tests that were done by targeting CLFLC liquid and/or mixed film lubricating and ILFLC boundary and/or mixed lubricating conditions were given at Figure 8,9 and  $\mu$  changes with W were given at Table 3. The friction values at both feeding tests were given at Figure 10. It was detected in all tests at both lubricating conditions (uncoated and MAO coated samples) that  $w$  was decreased with the increase of both velocity and load (Figure 10, Table 3). When friction performances at 50 N load in CLFLC was taken into hand, a bigger  $\mu$  value had gained at 0,438 m/s velocity while a lower  $\mu$  values were gained on MAO coated samples at 0,146 and 0,292 m/s sliding velocities compared to uncoated pin samples. The lowest  $\mu$  was carried out at 0.146 m/s sliding velocity at both uncoated and MAO coated tests at 100 N and 150 N loads.  $\mu$  was increased while MAO coating increased friction resistance. When W results of uncoated samples at both lubricating conditions, it was seen hat it was bigger compared to MAO coated samples and therefore friction resistance of MAO coating increased.

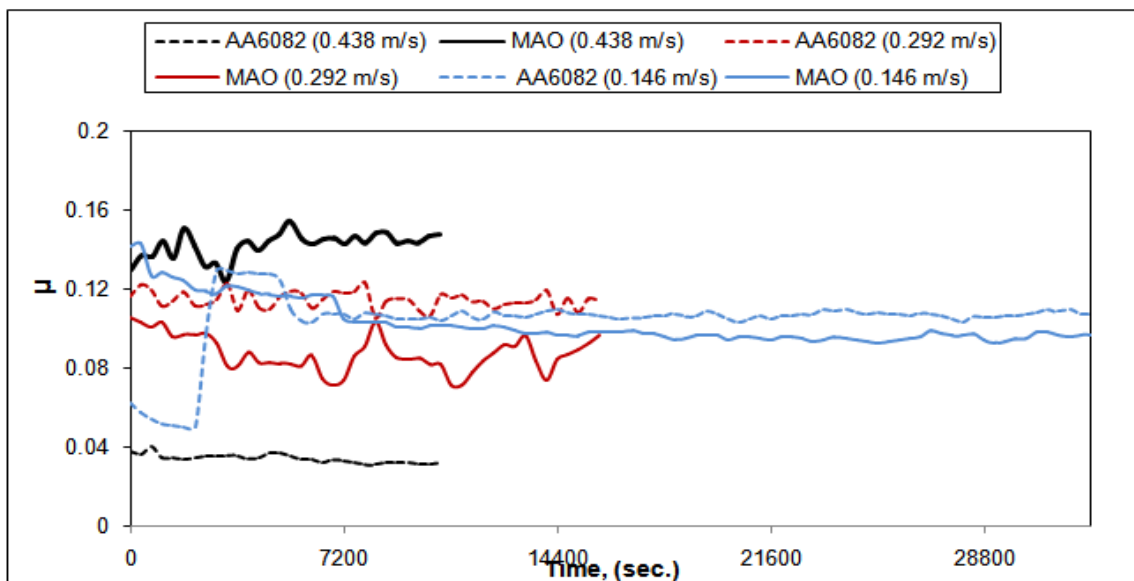


Figure 12.  $\mu$  change in CLFLC tests that were done in F=50 N



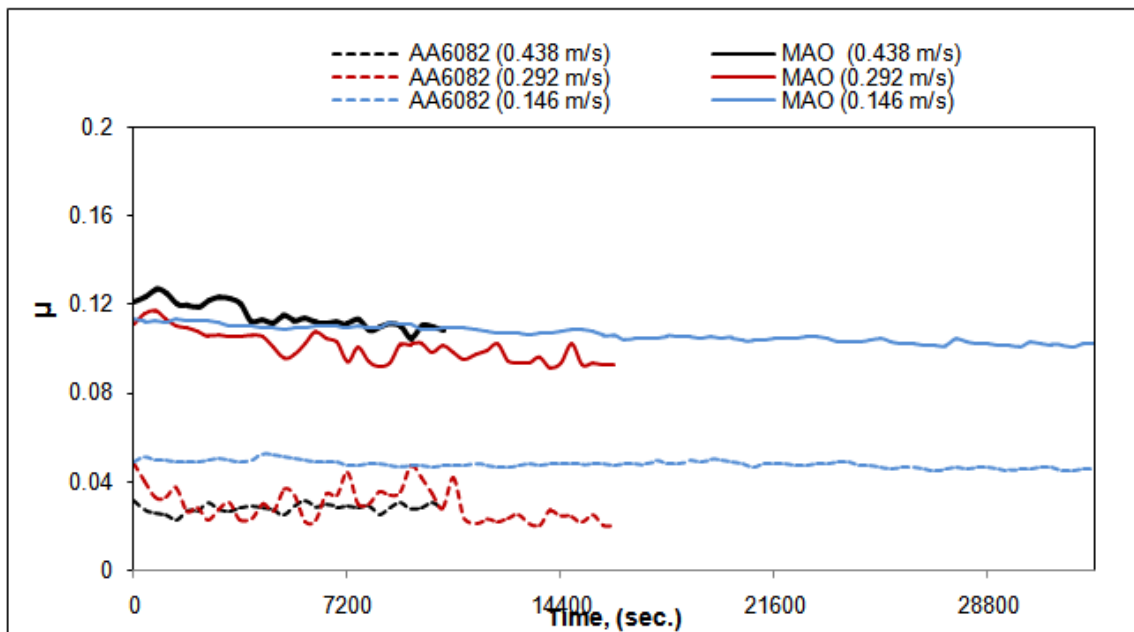


Figure 13.  $\mu$  change in CLFLC tests that were done in  $F=100$  N

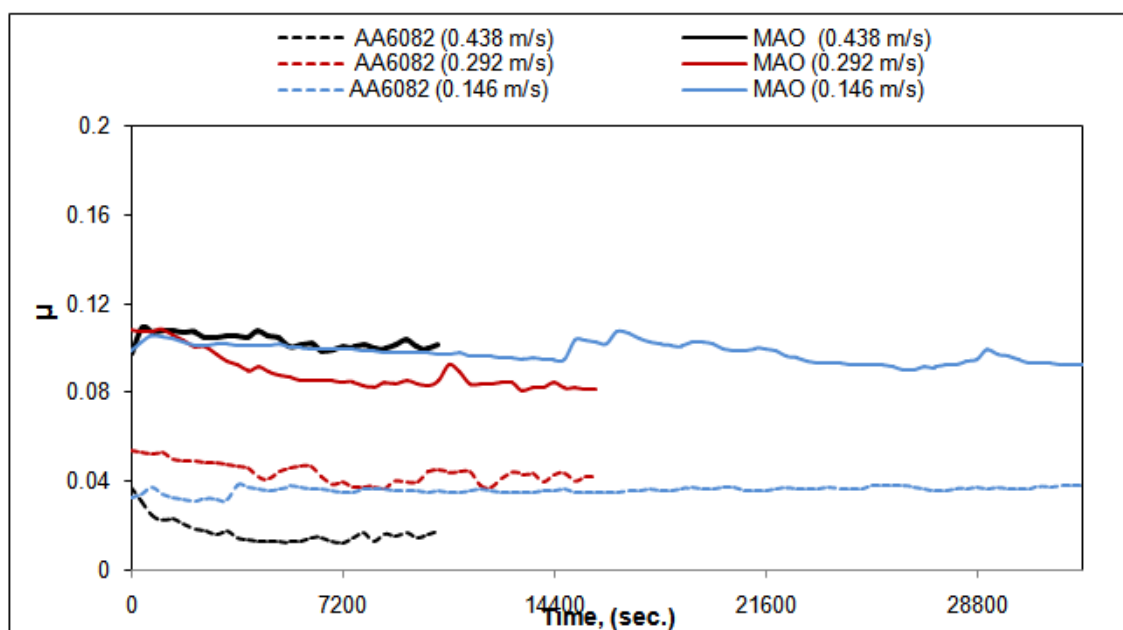


Figure 14.  $\mu$  change in CLFLC tests that were done in  $F=150$  N

Bigger values at both  $W$  and  $\mu$  were gained especially for uncoated samples at all load and velocities in ILFLC compared to the experiments done on CLFLC conditions (Table 3). Also while  $\mu$  values at especially 100 N and 150 N loads in MAO coated tests in ILFLC had downward trend at the end of the test, uncoated ones had showed less changing characteristic (Figure 9). While there was a general decrease even if average  $\mu$  was not tidy at the increase of both load and velocity in ILFLC uncoated tests, a big change was not observed with load and velocity increase of MAO coated sample. In both MAO coated and uncoated samples for both lubricating conditions, it was clearly seen in Figure 10 that friction amounts were increased with load increase at all experimental velocities. It is an indicator for better lubrication conditions in the tests at CLFLC conditions compared to ILFLC that a lower friction amount was gained.

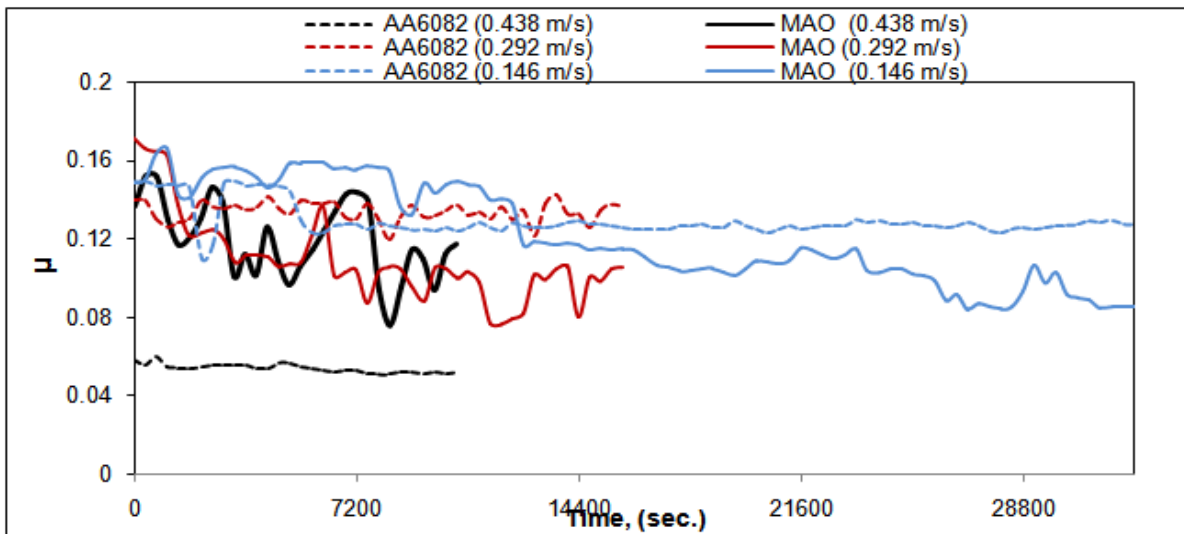


Figure 15.  $\mu$  change in ILFLC tests that were done in  $F=50$  N

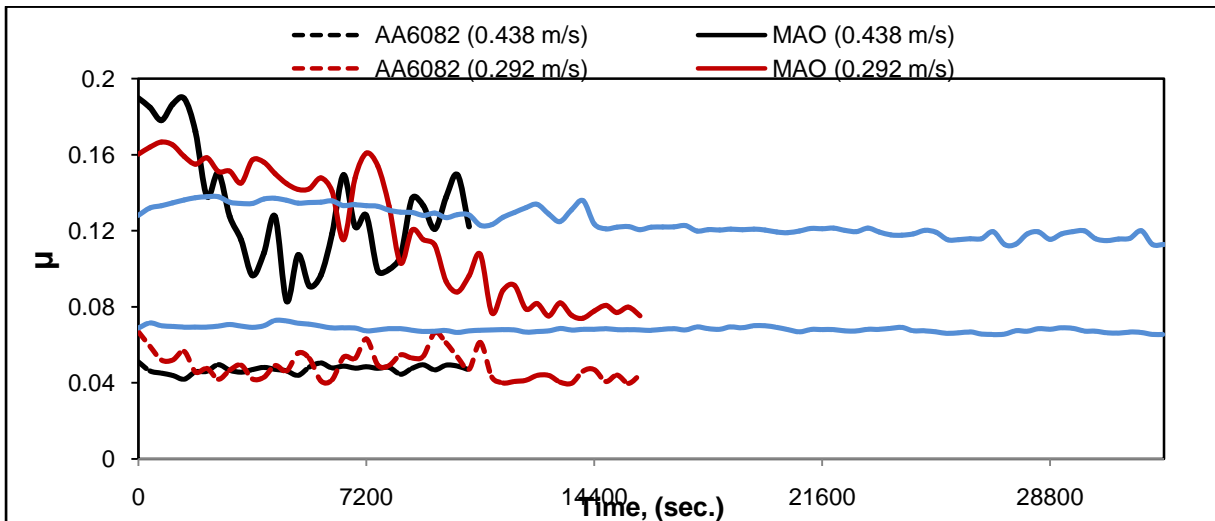


Figure 16.  $\mu$  change in ILFLC tests that were done in  $F=100$  N

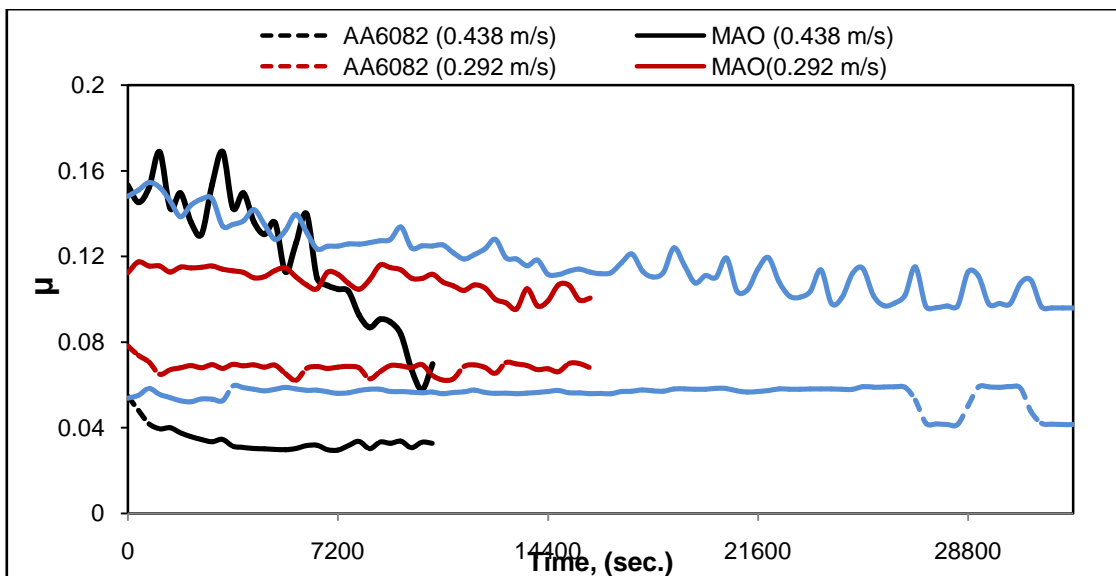
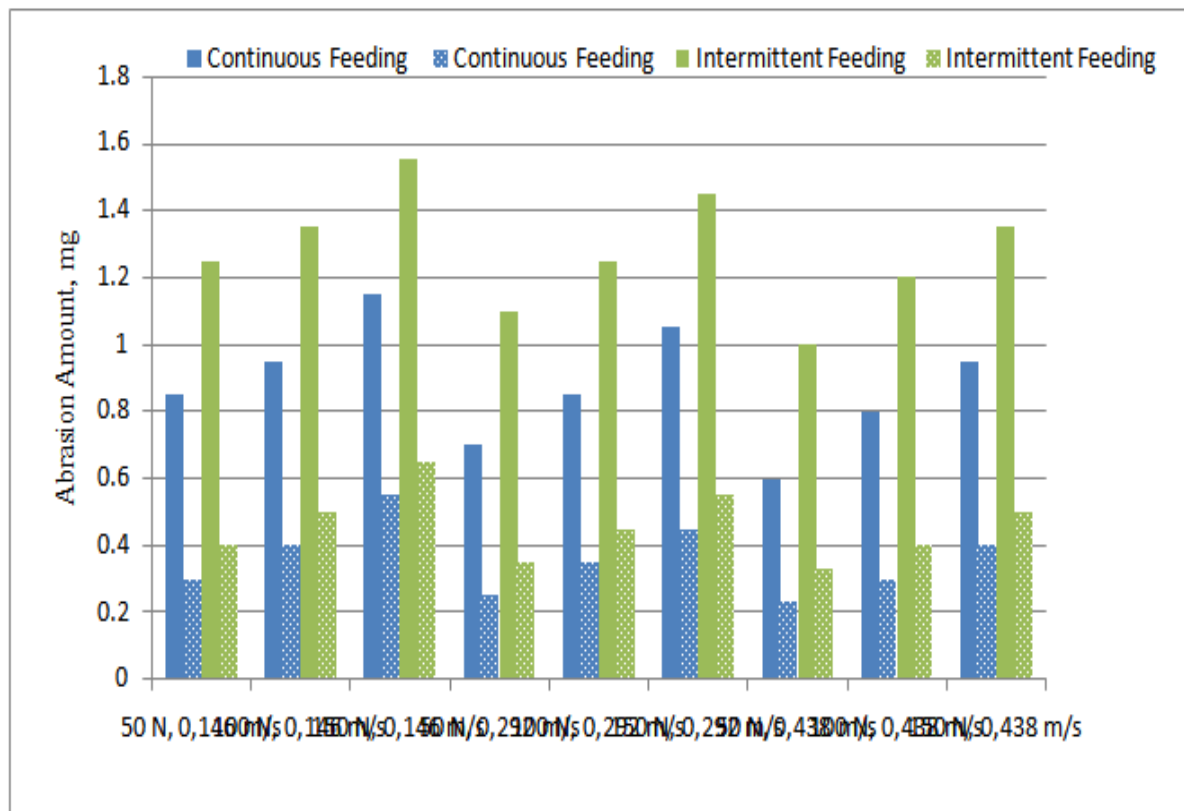


Figure 17.  $\mu$  change in ILFLC tests that were done in  $F=150$  N

**Table 3. Average  $\mu$  and W values at CLFLC and ILFLC in Pin Disc Wear Tests**

Load (N)	Velocity (m/s)	CLFLC				ILFLC			
		AA6082		MAO		AA6082		MAO	
		W( $10^{-17}$ )	$\mu$	W( $10^{-17}$ m <sup>3</sup> /Nm)	$\mu$	W( $10^{-17}$ m <sup>3</sup> /Nm)	$\mu$	W( $10^{-17}$ m <sup>3</sup> /Nm)	$\mu$
50	0,146	125,926	0,104	44,444	0,102	185,185	0,124	59,259	0,121
50	0,292	103,704	0,114	37,037	0,087	162,963	0,134	51,852	0,109
50	0,438	88,889	0,034	34,074	0,142	148,148	0,054	48,889	0,119
100	0,146	70,370	0,048	29,630	0,106	100,000	0,068	37,037	0,124
100	0,292	62,963	0,029	25,926	0,100	92,593	0,048	33,333	0,120
100	0,438	59,259	0,028	22,222	0,115	88,889	0,047	29,630	0,132
150	0,146	56,790	0,036	27,160	0,098	76,543	0,055	32,099	0,117
150	0,292	51,852	0,044	22,222	0,089	71,605	0,068	27,160	0,108
150	0,438	46,914	0,017	19,753	0,103	66,667	0,034	24,691	0,121

At SEM examinations of friction surfaces, friction traces of uncoated Pin samples at full load and velocities were more distinct and it was seen that bigger plastic deformation lines were formed due to that very small particles were separated from the materials at some parts and the velocity was increased. At MAO coated Pin samples, the friction traces were less distinct compared to uncoated Pin samples and this was especially seen at roughness tops of coating layer. As an example, surface examinations of the tests at 150 N load for both lubricating conditions are given in Figure 11 and 12.



**Figure 18. The friction amount in the tests at CLFLC and ILFLC conditions in Pin Disc tests**

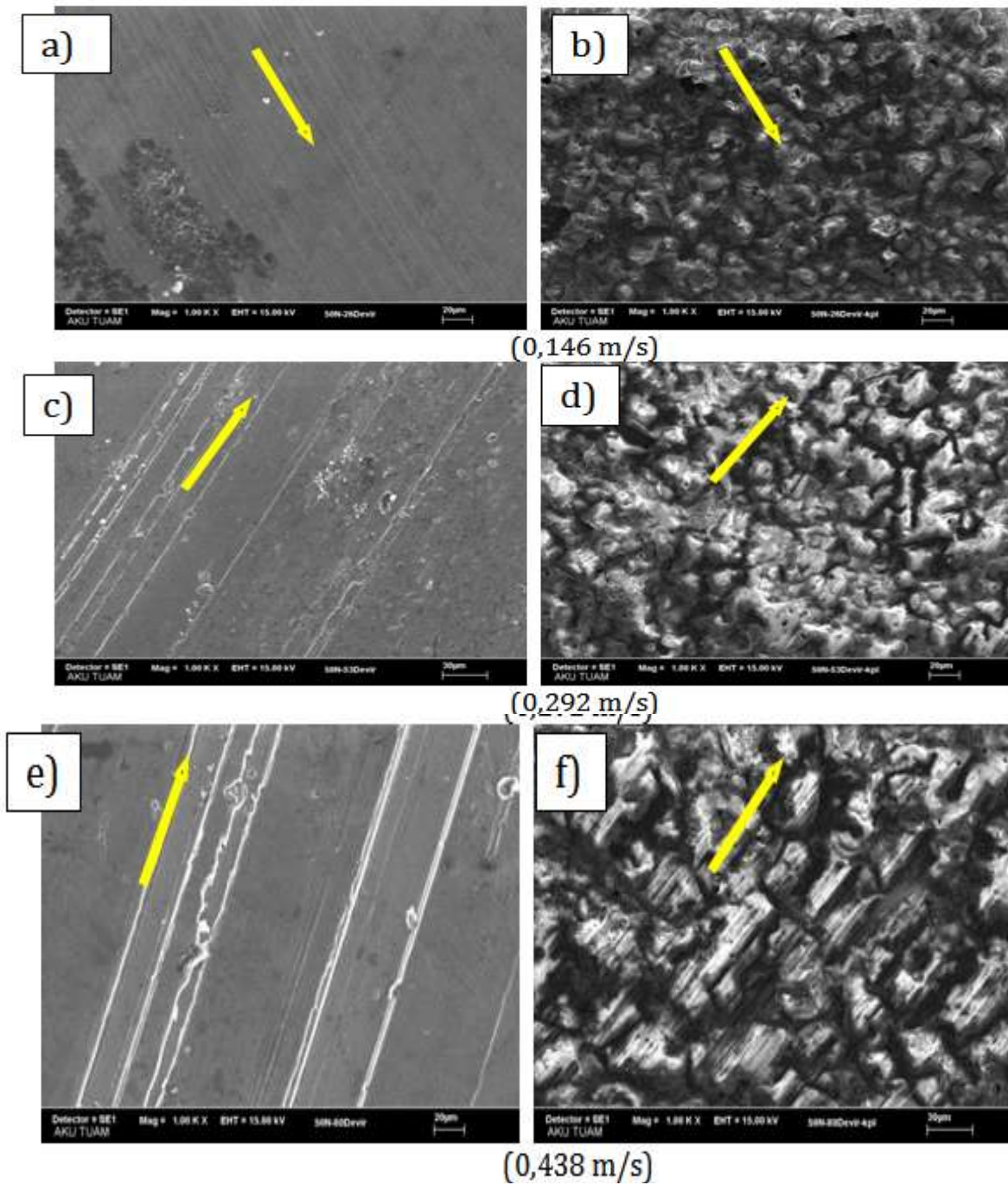


Figure 19. Uncoated (a;c;e) and MAO coated (b;d;f) SEM images at 50 N load in CLFLC

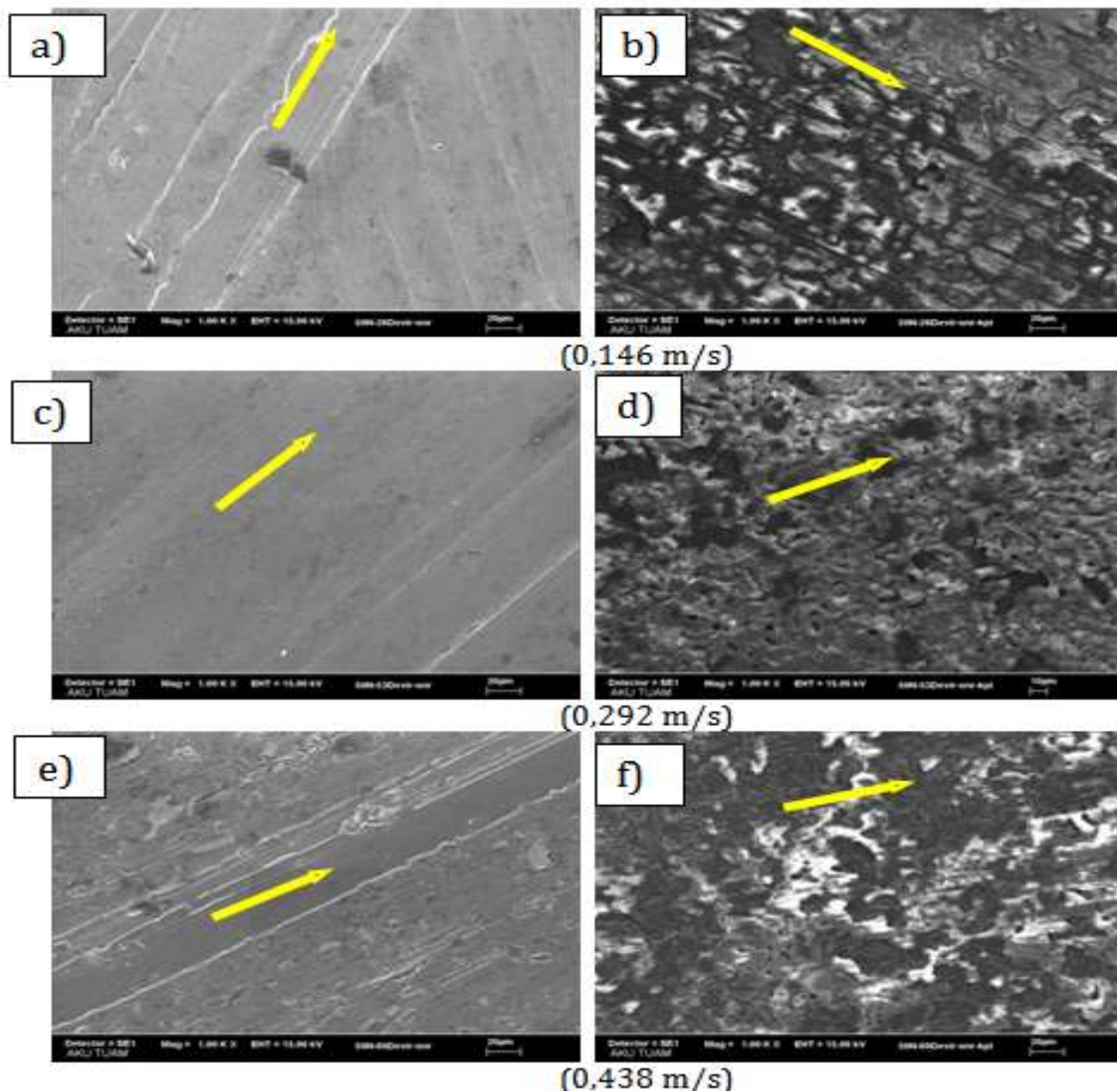


Figure 20. Uncoated (a;c;e) and MAO coated (b;d;f) SEM images at 50 N load in ILFLC

### 3.7. Continuous and Intermittent Lubricant Feeding Test Results at RTR

The experiments were done in CLFLC and ILFLC at Reciprocating Test Apparatus. The  $\mu$  changes that were obtained under these conditions are given at Figure 13,14 and changes of  $W$  and  $\mu$  are given at Table 3. Also the abrasion amounts at both feeding tests are given at Figure 15. As in Pin Disc abrasion tests,  $W$  was decreased at both uncoated and MAO coated samples at all loads and all velocities under both lubricating conditions in reciprocating tests with the increase of both velocity and load and therefore abrasion resistance of MAO coating was increased (Figure15.Table3). When friction performances at all loads under both lubricating conditions were reviewed, average  $\mu$  was decreased with the increase of velocity at uncoated Pin samples, an increase even at small amount was observed at MAO coated samples. As in Pin Disc abrasion tests, a bigger values were obtained both in terms of  $W$  and  $\mu$  at all loads and velocities in ILFLC of reciprocating tests compared to the experiments that were done on especially uncoated samples in CLFLC (Table 3). This is the indicator of that the lubricating conditions were better in CLFLC tests compared to ILFLC. It may be clearly seen in Figure 15 that abrasion amounts were increased with load increase at all experiment velocities on both MAO coated and uncoated samples for both lubricating conditions.

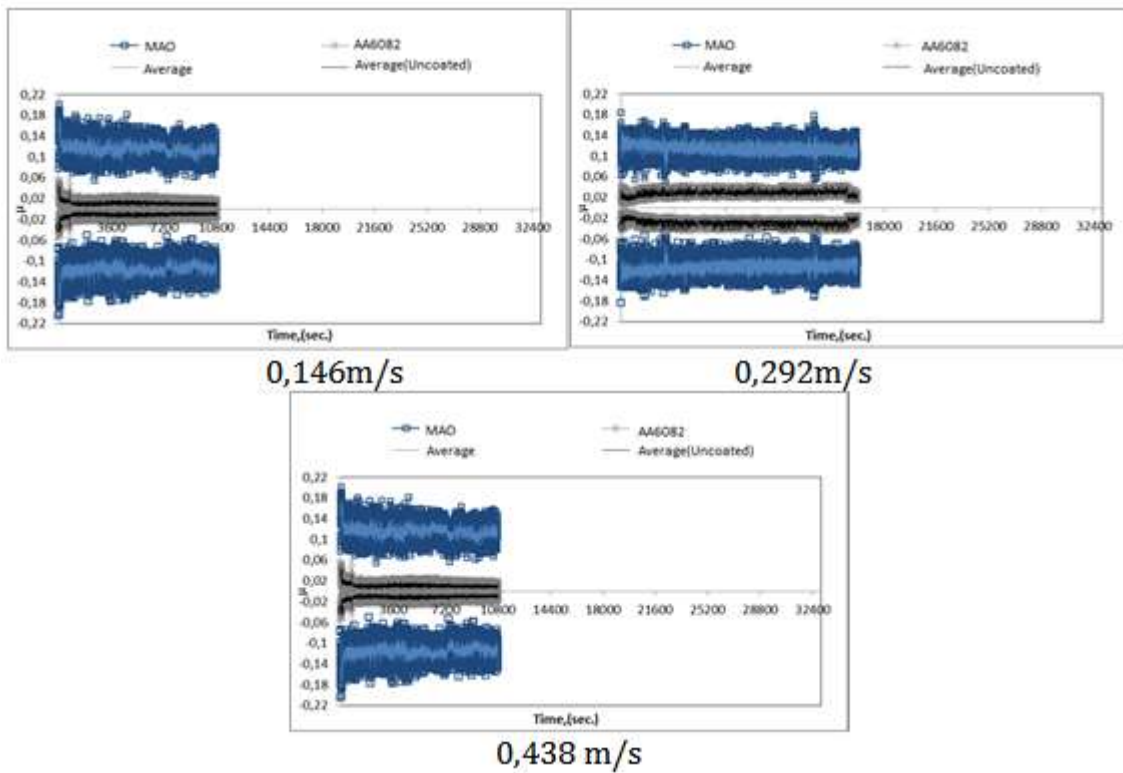


Figure 21.  $\mu$ change in CLFLC at F=50 N

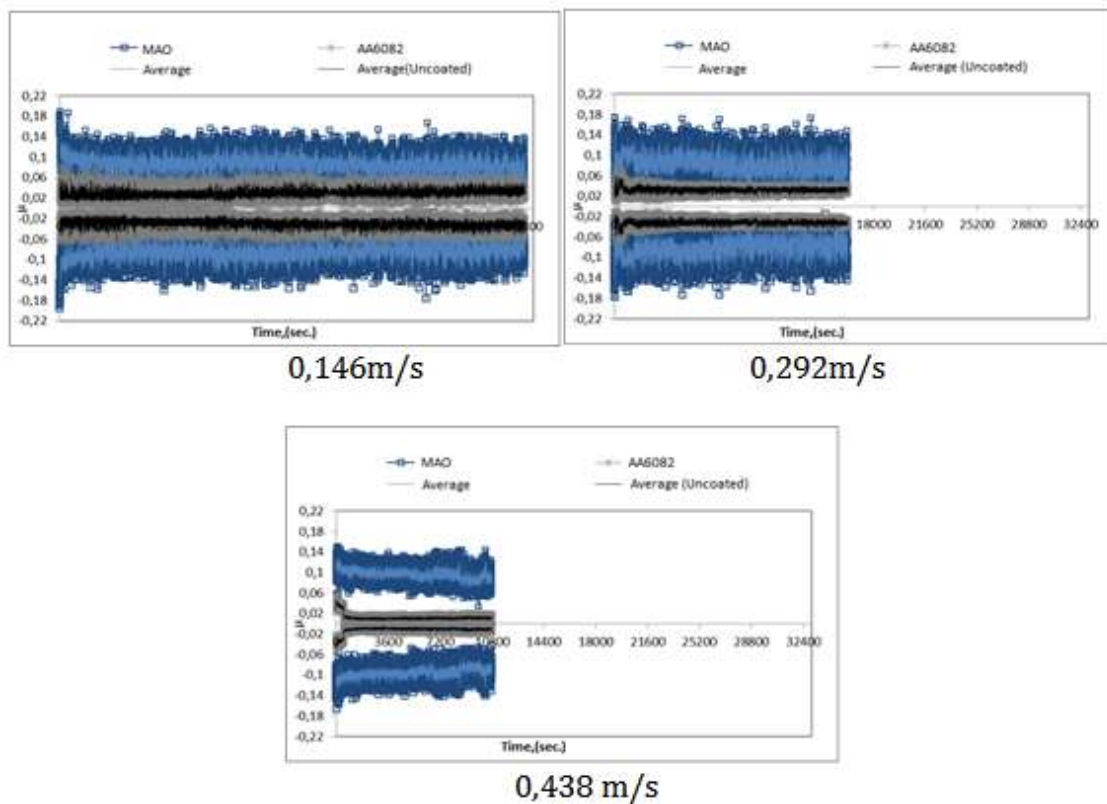


Figure 22.  $\mu$ change in CLFLC at F=100 N

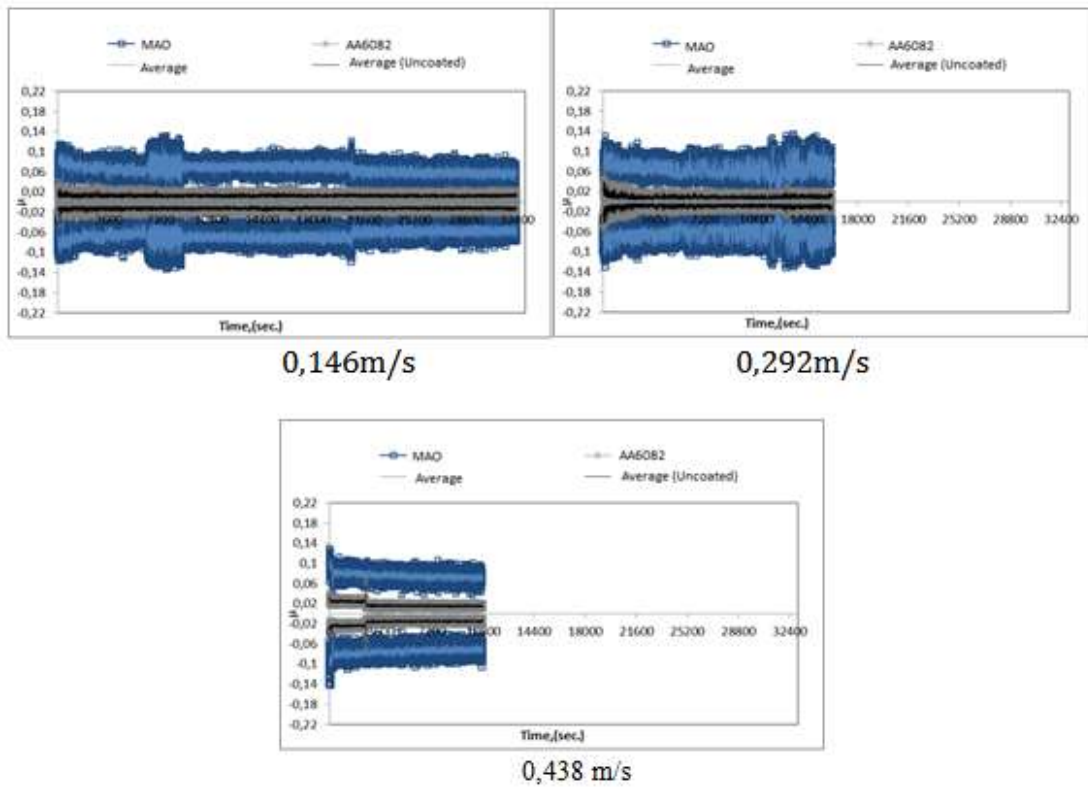


Figure 23.  $\mu$ change in CLFLC at F=150 N

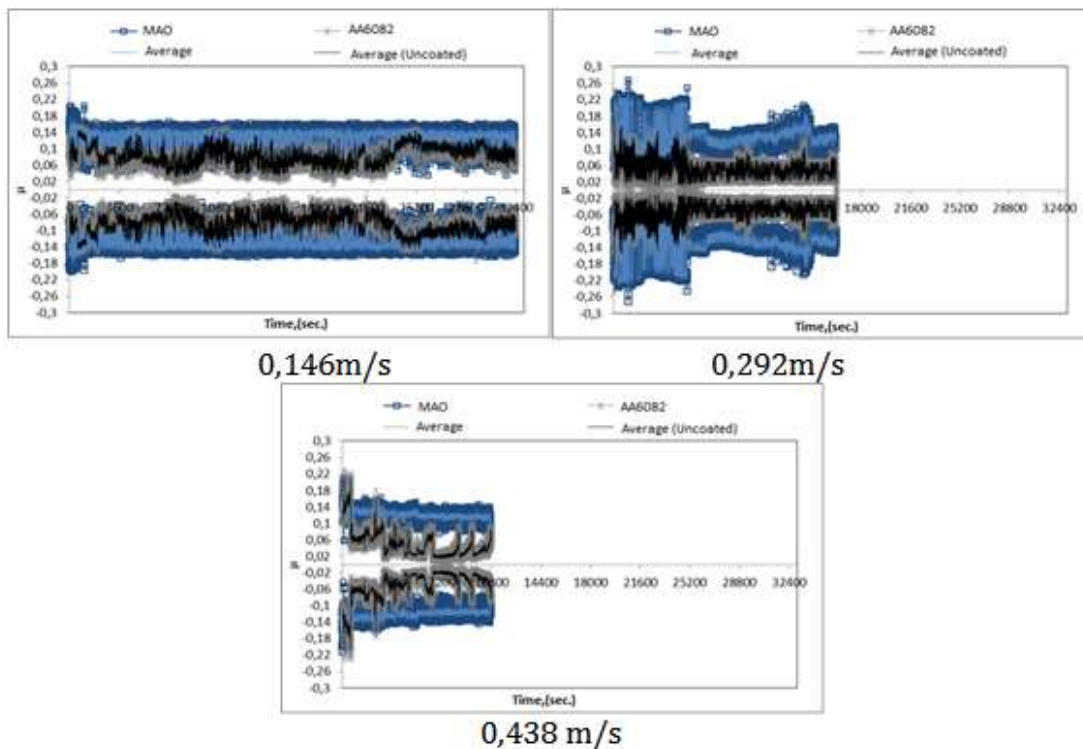


Figure 24.  $\mu$ change in ILFLC at F=50 N

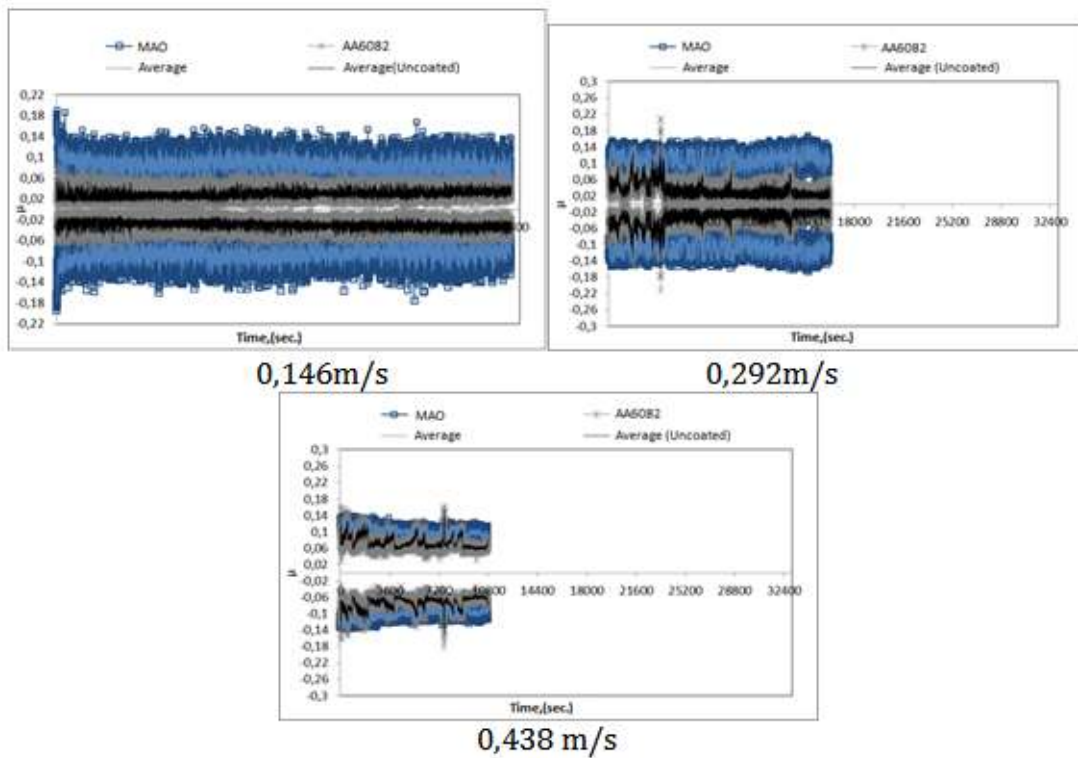


Figure 25.  $\mu$  change in ILFLC at F=100 N

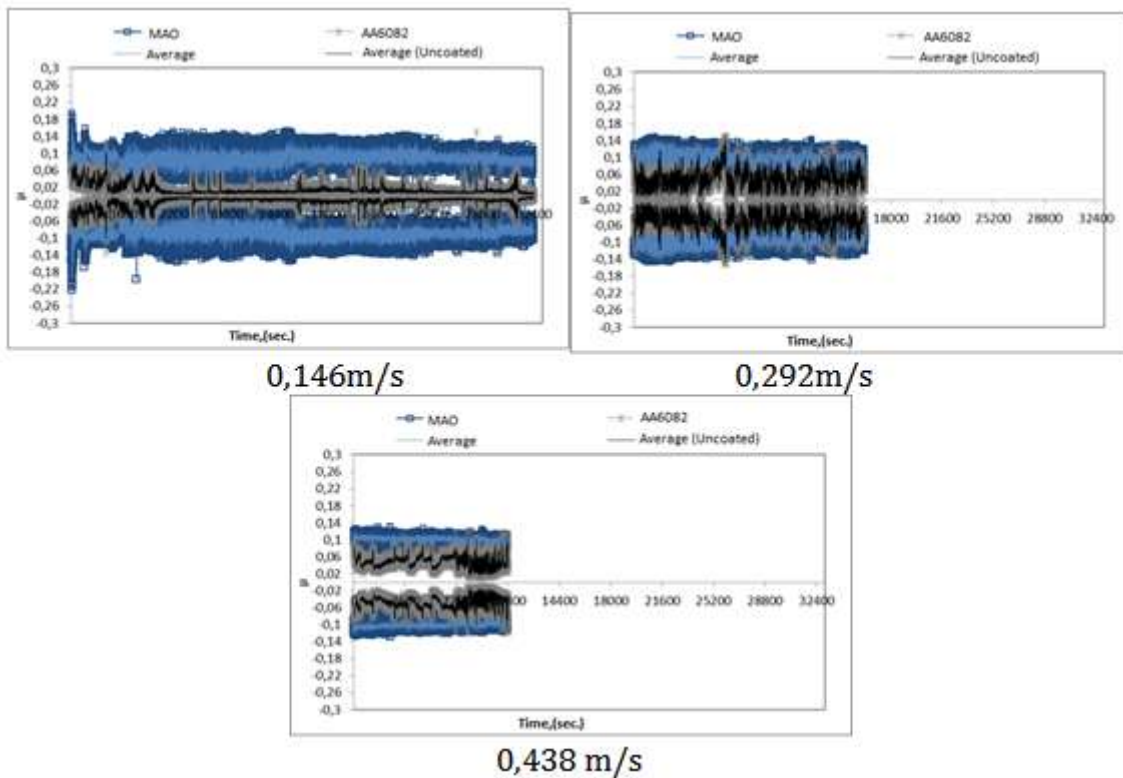
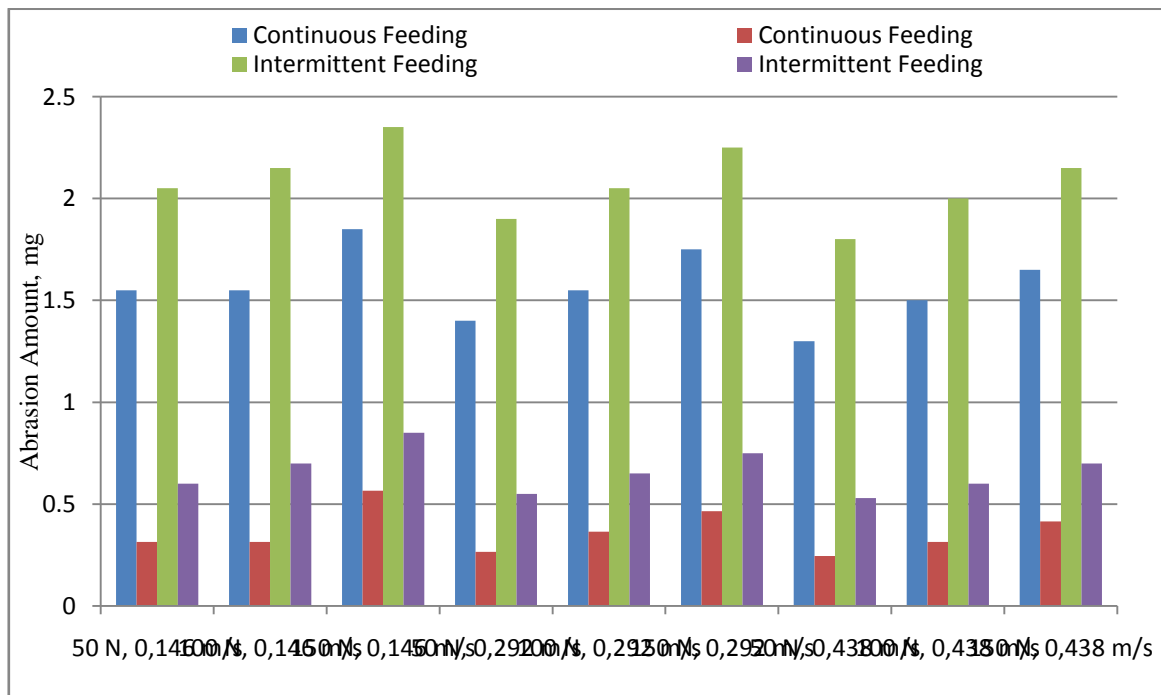


Figure 26.  $\mu$  change in ILFLC at F=150 N



**Table 4. Average  $\mu$  and W values in CLFLC and ILFLC at Reciprocating Test Device**

Load (N)	Velocity (m/s)	CLFLC				ILFLC			
		AA6082		MAO		AA6082		MAO	
		W( $10^{-17}$ )	$\mu$	W( $10^{-17}$ m <sup>3</sup> /Nm)	$\mu$	W( $10^{-17}$ m <sup>3</sup> /Nm)	$\mu$	W( $10^{-17}$ m <sup>3</sup> /Nm)	$\mu$
50	0,146	229,630	0,052	46,667	0,100	303,704	0,084	88,889	0,127
50	0,292	207,407	0,028	39,259	0,115	281,481	0,053	81,481	0,129
50	0,438	192,593	0,010	36,296	0,116	266,667	0,050	78,519	0,121
100	0,146	122,222	0,029	30,741	0,087	159,259	0,050	51,852	0,121
100	0,292	114,815	0,032	27,037	0,082	151,852	0,033	48,148	0,110
100	0,438	111,111	0,011	23,333	0,096	148,148	0,079	44,444	0,102
150	0,146	91,358	0,012	27,901	0,065	116,049	0,014	41,975	0,087
150	0,292	86,420	0,009	22,963	0,064	111,111	0,048	37,037	0,094
150	0,438	81,481	0,017	20,494	0,075	106,173	0,047	34,568	0,101



**Figure 27. The abrasion amount in CLLC and ILFLC in reciprocating test**

It was clearly seen in Figure 15 that abrasion amounts were increased with the increase of load at all experiment velocities in both MAO coated and uncoated samples for both lubricating conditions. Obtaining a lower abrasion amount in CLFLC tests compared to ILFLC may be the indicator for that lubricating conditions were better.

At the SEM examinations of abrasion surfaces, it was seen that abrasion traces were more distinct on uncoated Pin samples at load and velocities and very small particles were pulled out from the material at some parts. At MAO coated Pin samples, it was seen that abrasion traces of uncoated Pin samples were at very small amounts and especially seen at roughness tops of the coating layer. Surface examinations of the tests at 50 N load for both lubricating conditions were given at Figure 16 and Figure 17.

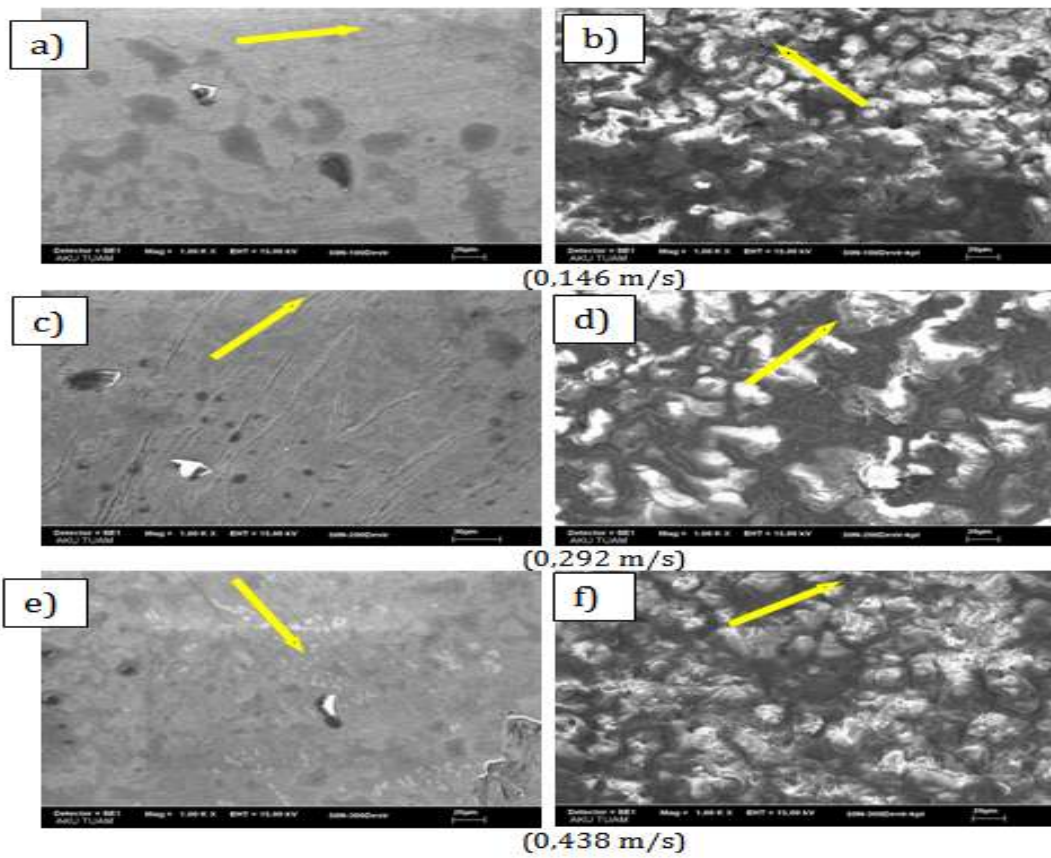


Figure 28. Uncoated (a;c;e) and MAO coated (b;d;f) SEM images at 50 N load in CLFLC

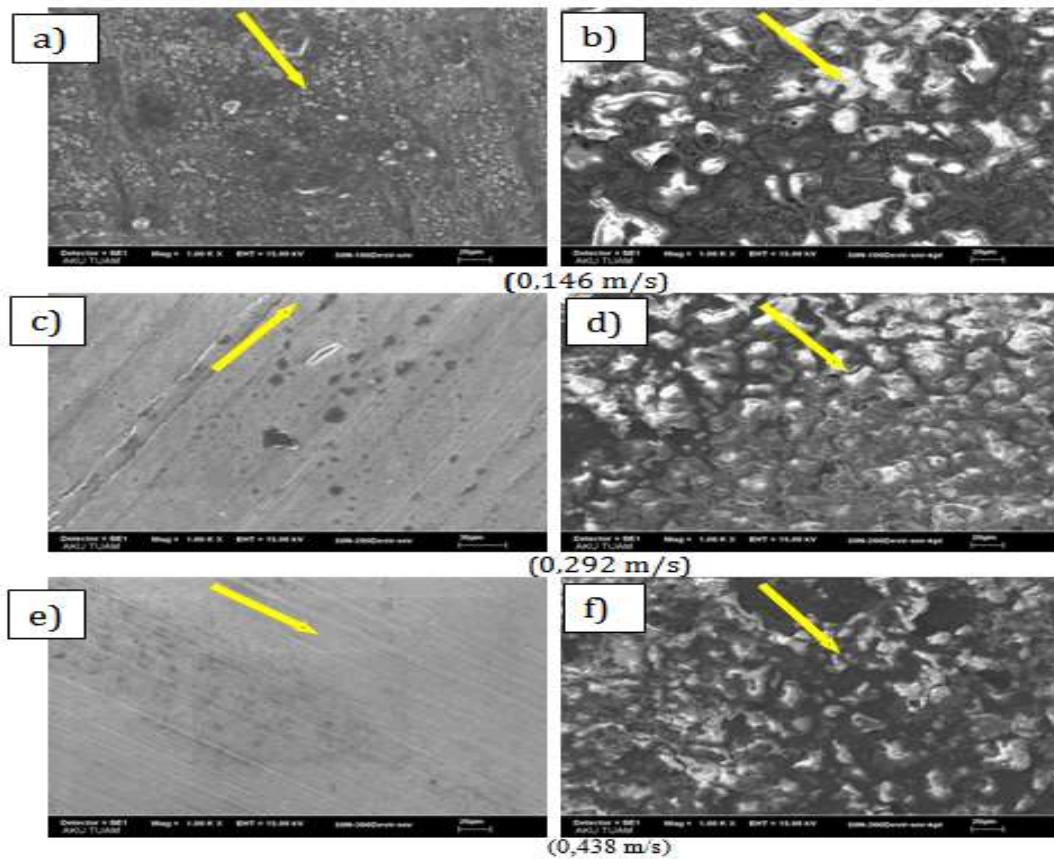


Figure 29. Uncoated (a;c;e) and MAO coated (b;d;f) SEM images at 50 N load in ILFLC

As in the test result of PDWTR; even if surface roughness of coated sample at both lubricating conditions in reciprocating tests (Table 4, 5, 6, 7) was higher, a lower friction was formed at the material. This may be bound to that hardness of coating layer at the surface was higher compared to AA6082. It was thought that bigness of  $\mu$  in MAO coated tests led to bigness of the roughness at these samples (Table 3) and interlocking of these roughness led to increase  $\mu$ . Also coated and uncoated Pin samples at both lubricating conditions showed a reduction in average roughness values even if at different amounts after the experiment (Table3).

Also as in the test result of PDWTR; it is thought that they were exposed to a more severe working conditions as PV factor at MAO coated samples were bigger compared to uncoated samples (Table 4, 5, 6, 7) at both of the lubricating conditions in RTR and therefore this may lead to that  $\mu$  value of MAO coated samples were higher compared to  $\mu$  values of uncoated samples. It was seen that sufficient and continuous a lubricant film was not formed even if lubricant was sent continuously in CLFLC. The roughness tops being very big may lead to tear of the lubricant film and/or its being insufficient in terms of filling the roughness pits. If an amount of stoning and/or polishing procedures were done for lowering heights of big roughness tops of the test samples' surfaces after the coating procedure, it was thought that a better lubricating condition may be formed. Therefore when bigness of  $\mu$  values gained in this study was taken into hand, it was understood that it was a boundary lubricating[22]. A bigger abrasion contact percentage was formed due to insufficient lubricating and  $\mu$  was increased because of big roughness tops due to mechanical capture. A bigger PV factor was detected at all experiments of both uncoated and MAO coated experiments in CLFLC compared to ILFLC. A more effective lubricating was occurred with effect of CLFLC compared to ILFLC and as a result of this, a lower abrasion surface was formed.

As there are many micropores, microcracks and dimples on the surface of the MAO coatings, these pores, cracks and dimples can act as reservoirs for oil lubricants, which may result in a positive effect to the tribological performance of MAO coatings under boundary-lubricated conditions[9].

Fei Zhou et al[23]investigated the friction characteristic of MAO coating on AA2024 alloy, sliding against  $\text{Si}_3\text{N}_4$  balls, in water and oil environments, at different normal loads and sliding speeds. Results showed that, with the increasing of normal load and sliding speed, the friction coefficient of the MAO/ $\text{Si}_3\text{N}_4$  tribopair in water and oil decreased from 0.72 to 0.57 and 0.24 to 0.11 respectively. The wear mechanism of the MAO coatings changed from abrasive wear in air to mix wear in water, and finally became microploughing wear in oil[9].

When the wearing performances (both W and wearing amount) were taken into consideration, it was seen that the results of reciprocating test set was bigger compared to the tests results of PDWTR. The reason of this is that while there was a one way sliding movement in the PDWTR, RTR was two way and as it behaved like a rasping procedures, it removes the roughness available on the surface and therefore made much more friction. It was seen that friction amount was increased at both uncoated and MAO coated samples with the increase of the load (Figure 14). It was thought that sometimes two body and sometimes three body abrasive abrasion type (Figure 18) was formed in the tests and surface examinations. Until recently these two modes of abrasive wear thought to be very similar, however, some significant differences between them have been revealed. It was found that three-body abrasive wear is ten times slower than two-body wear since it has to compete with other mechanism such as adhesive wear. Two-body abrasive wear corresponds closely to the 'cutting tool' model of material removal whereas three-body abrasive wear involves slower mechanisms of material removal, though very little is known about the mechanisms involved. This may be explained with that worn particles behaved as ball and they pulled off particles from the surface[24,25].

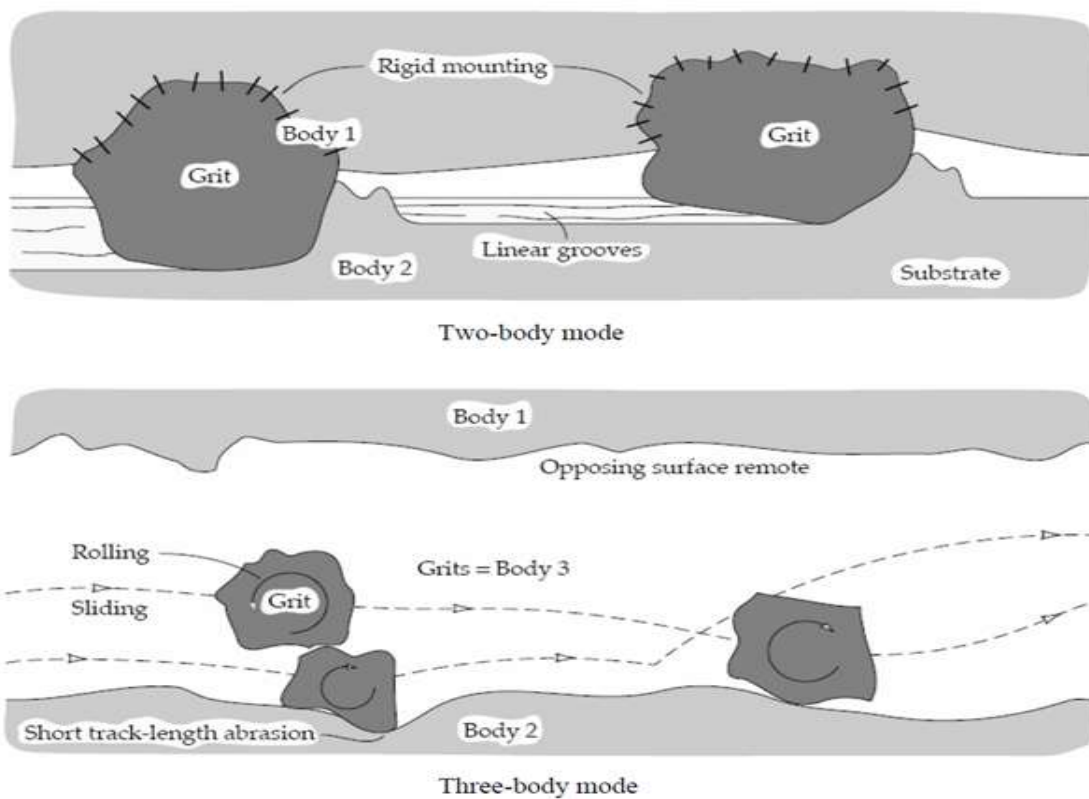


Figure 30. Two and three-body of abrasive ((Blanchett and Kennedy, 1989)(

Why the friction ratio was lower at MAO coated sample and as well as that  $\mu$  level was high may be explained with that liquid and lubricant was not completely regained at the surfaces, metal-metal contact and roughness were interlocked due to insufficient lubricating conditions. This means that mixed and/or boundary lubricating conditions were available here. Malayoglu et al. (2011) pointed out the lubricating film effectively delays the wear process by redistributing the stresses over a larger area as well as by removing the strain as a result of film wear. This film can be easily removed, thereby providing a low-shear interfacial layer against the rubbing. So, instead of the surface being worn away, it is the film layer that is removed. If we consider the surface morphology of coating, the micro-pores present on the surface acted as oil reservoirs and contributed to the bonding of lubricating film. Thus the stability of lubricating film is increased during sliding[26]

Table 5. PV factor, average roughness values in lubricant experiments that were done in Pin on Disc Abrasion Test Apparatus( $R_a$ ,  $\mu\text{m}$ ) (CLFLC)

Load (N)	Velocity (m/s)	MAO ( $R_a$ , $\mu\text{m}$ )			AA6082 ( $R_a$ , $\mu\text{m}$ )			MAO ( $R_a$ , $\mu\text{m}$ )		AA6082 ( $R_a$ , $\mu\text{m}$ )	
		Measured Contact Area ( $\text{mm}^2$ )	P (MPa)	P.V (MPa.m/s)	Measured Contact Area ( $\text{mm}^2$ )	P (MPa)	P.V (MPa.m/s)	Before the Experiment	After the Experiment	Before the Experiment	After the Experiment
50	0.146	3,144	15,923	2,324	5,495	9,099	1,328	2,864	1,897	0,568	0,471
50	0.292	3,147	15,923	4,649	3,925	12,738	3,719	2,920	2,583	0,789	0,723
50	0.438	3,925	12,738	5,579	3,925	12,738	5,579	2,418	1,749	0,441	0,351
100	0.146	3,924	25,477	3,719	7,065	14,154	2,066	3,020	2,941	0,620	0,504
100	0.292	4,718	21,231	6,199	6,281	15,923	4,649	2,671	2,015	0,718	0,633
100	0.438	3,925	25,477	11,159	5,495	18,198	7,970	2,220	1,698	0,568	0,496
150	0.146	7,065	21,231	3,099	9,426	15,923	2,324	2,678	2,209	0,457	0,224
150	0.292	5,495	27,297	7,970	7,852	19,108	5,579	2,418	2,070	0,612	0,451
150	0.438	4,716	31,847	13,949	7,065	21,231	9,299	2,675	2,271	0,465	0,304

**Table 6. PV factor in the experiments that were done in Pin on Disc Abrasion Test Apparatus(MAO coated ILFLC)**

Load (N)	Velocity (m/s)	MAO ( $R_a$ , $\mu\text{m}$ )			AA6082 ( $R_a$ , $\mu\text{m}$ )			MAO ( $R_a$ , $\mu\text{m}$ )		AA6082 ( $R_a$ , $\mu\text{m}$ )	
		Measured Contact Area ( $\text{mm}^2$ )	P (MPa)	P.V (MPa.m/s)	Measured Contact Area ( $\text{mm}^2$ )	P (MPa)	P.V (MPa.m/s)	Before the Experiment	After the Experiment	Before the Experiment	After the Experiment
50	0,146	7,065	7,077	1,033	7,851	6,369	0,929	2,200	1,236	0,498	0,448
50	0,292	8,635	5,790	1,690	9,427	5,307	1,549	2,150	1,015	0,765	0,72
50	0,438	13,345	3,746	1,641	15,701	3,184	1,394	2,382	1,375	0,523	0,318
100	0,146	7,851	12,738	1,859	11,715	8,492	1,239	2,415	1,420	0,782	0,733
100	0,292	15,703	6,369	1,859	15,700	6,369	1,859	2,510	0,891	0,428	0,257
100	0,438	18,055	5,538	2,425	19,625	5,095	2,231	2,672	1,328	0,412	0,151
150	0,146	11,775	12,738	1,859	23,509	6,369	0,929	2,227	1,060	0,460	0,157
150	0,292	15,798	9,554	2,789	35,305	4,246	1,239	2,417	1,287	0,678	0,317
150	0,438	23,556	6,369	2,789	31,408	4,777	2,092	2,228	0,719	0,511	0,179

**Table 7. PV factor in the experiments that were done in Reciprocating Abrasion Test Apparatus (MAO coated CLFLC)**

Load (N)	Velocity (m/s)	MAO ( $R_a$ , $\mu\text{m}$ )			AA6082 ( $R_a$ , $\mu\text{m}$ )			MAO ( $R_a$ , $\mu\text{m}$ )		AA6082 ( $R_a$ , $\mu\text{m}$ )	
		Measured Contact Area ( $\text{mm}^2$ )	P (MPa)	P.V (MPa.m/s)	Measured Contact Area ( $\text{mm}^2$ )	P (MPa)	P.V (MPa.m/s)	Before the Experiment	After the Experiment	Before the Experiment	After the Experiment
50	0,146	10,996	4,549	0,664	74,575	0,670	0,097	2,201	1,700	0,445	0,085
50	0,292	4,715	10,611	3,099	33,755	1,481	0,432	2,670	2,262	0,620	0,034
50	0,438	18,840	2,653	1,162	25,121	1,990	0,871	2,520	1,633	0,568	0,048
100	0,146	11,775	8,492	1,239	78,509	1,273	0,185	2,765	1,669	0,582	0,028
100	0,292	17,271	5,790	1,690	35,325	2,830	0,826	2,787	1,608	0,612	0,068
100	0,438	20,415	4,899	2,146	23,554	4,246	1,859	2,715	1,113	0,427	0,051
150	0,146	15,706	9,554	1,394	78,517	1,910	0,278	2,563	1,451	0,530	0,036
150	0,292	14,134	10,615	3,099	78,509	1,910	0,557	2,487	1,168	0,545	0,048
150	0,438	35,325	4,246	1,859	29,834	5,028	2,202	2,586	1,268	0,615	0,058

**Table 8. PV factor in the experiments that were done in Reciprocating Abrasion Test Apparatus (Uncoated ILFLC)**

Load (N)	Velocity (m/s)	MAO ( $R_a$ $\mu\text{m}$ )			AA6082 ( $R_a$ $\mu\text{m}$ )			MAO ( $R_a$ $\mu\text{m}$ )		AA6082 ( $R_a$ $\mu\text{m}$ )	
		Measured Contact Area ( $\text{mm}^2$ )	P (MPa)	P.V (MPa.m/s)	Measured Contact Area ( $\text{mm}^2$ )	P (MPa)	P.V (MPa.m/s)	Before the Experiment	After the Experiment	Before the Experiment	After the Experiment
50	0,146	23,55	2,123	0,309	72,2	0,692	0,101	2,120	1,253	0,561	0,501
50	0,292	4,710	10,615	3,099	54,9	0,909	0,265	2,370	1,612	0,415	0,199
50	0,438	23,55	2,123	0,929	78,5	0,636	0,278	2,481	1,246	0,492	0,101
100	0,146	19,625	5,095	0,743	54,9	1,8193	0,265	2,313	1,089	0,626	0,414
100	0,292	10,205	9,799	2,861	78,5	1,273	0,371	2,317	1,331	0,429	0,091
100	0,438	19,625	5,095	2,231	78,5	1,273	0,557	2,377	1,459	0,517	0,126
150	0,146	36,119	4,153	0,606	78,5	1,9108	0,278	2,510	0,954	0,623	0,112
150	0,292	15,705	9,554	2,789	78,5	1,9108	0,557	2,426	1,350	0,587	0,127
150	0,438	33,755	4,443	1,946	78,5	1,9108	0,836	2,414	1,271	0,552	0,110

#### IV. CONCLUSIONS

- By applying a fixed current to AA6082 alloy in  $\text{KOH}+\text{Na}_2\text{SiO}_3$  solution approximately for 30 minutes, the samples were coated with MAO procedure. This coating layer was formed Al and  $\gamma\text{-Al}_2\text{O}_3$  phases of porous oxide layer.
- It was clearly seen in this study as stated in the literature that a porous external region was formed in the coating and more frequent a layer and a fine inter surface region was formed under this layer. The thickness measurements were approximately  $29 \pm 2 \mu\text{m}$  and it was seen that this was close to the similar studies available in the literature. A more rough structure was obtained.
- When AA6082 material is coated with MAO in the measurements, about ten times more increase was detected at hardness values. This increased hardness value made a positive significant resistance to abrasion resistance.
- It was detected that the abrasion ratios of working surface in the experiments done in CLFLC were lower compared to coated samples.
- It was detected that W was decreased with the increase of load and velocity on MAO coated and uncoated samples in CLFLC and ILFLC.
- $\mu$  at coated samples were detected as higher compared to uncoated ones and the reason of this may be that a sufficient lubricant film was not completely formed between the contact surfaces available between Pin and opposite surface even if feeding is done with liquid lubricant. It is thought that big roughness available on the surfaces may lead to this.
- Also PV value at MAO coated samples that have a very practical importance in the systems working equal to each other is bigger compared to PV value of uncoated samples. It is thought that Pin and opposite surface working equally to each other are subjected to the severe working conditions and therefore this may be lead to bigger  $\mu$  value at coated MAO samples.
- In the experiments that were done under boundary lubricating conditions in ILFLC, it was detected that  $\mu$  at MAO coated samples were higher compared to uncoated ones. It was detected that W was lower at MAO coated samples compared to uncoated samples.
- When abrasion performances (both W and abrasion amount) were reviewed, it was seen that they were bigger in the tests done at RTR compared to the test results of PDWTR. The reason of this is that while one way sliding movement occurs at PDWTR, this is two ways in RTR.
- It is thought that better lubricating conditions may be obtained if an amount of stoning and/or polishing procedure is done after surface coating procedure of MAO coated AA6082 samples.

## ACKNOWLEDGEMENT

We thank to Süleyman Demirel University Directorate of Scientific Research Projects Management Department that supports my thesis financially with Scientific Research Project No 3288-D1-12.

## REFERENCES

- [1]. Gaoa, H., Meng Zhanga, Xin Yangb, Ping Huangc, Kewei Xu.: Effect of  $\text{Na}_2\text{SiO}_3$  solution concentration of micro-arc oxidation process on lap-shear strength of adhesive-bonded magnesium alloys, *Applied Surface Science* 314, 447–452. (2014)
- [2]. Krishna, L. R., Somaraju, K.R.C., Sundararajan, G.: The Tribological Performance Of Ultra-Hard Ceramic Composite Coatings Obtained Through Microarc Oxidation. *Surface and Coatings Technology*. 163-164, 484-490. (2003)
- [3]. Kalkancı, H.: Plazma Elektrolitik Oksidasyon Teknolojisi Uygulanan AA6082 Alaşımının Özelliklerinin Araştırılması. Sakarya University, Institute of Science and Technology, Master's Thesis, 211s, Sakarya (2008)
- [4]. Arslan, E., Totik, Y., Alasaran, A., Demirci, E.E.: Plazma Elektrolitik Oksidasyon Yöntemi ile Alüminyum, Magnezyum ve Titanyum Alaşımlarının Yüzey Modifikasyonu: Aşınma ve Korozyon Özelliklerinin Araştırılması. Tübitak project no: 107 M313, 95s. (2009)
- [5]. Butyagin, P.X., Ramazonova, J.M., Khokhryakov, Y.V., Budnitskayab, Y.Y., Mamaev, A.: Industrial Application of Coatings Formed by Microarc Oxidation Euromat, Lausanne( 2003)
- [6]. Krishna, L.R., Gupta, P.S.V.N.B., Sundararajan, G.: The influence of phase gradient within the micro arc oxidation (MAO) coatings on mechanical and tribological behaviors. *Surface & Coatings Technology*, 269, 54–63. (2015)
- [7]. Dunleavy C.S., I.O. Golosnoy b, J.A. Curran a,c, T.W. Clyne.: Characterisation of discharge events during plasma electrolytic oxidation. *Surface & Coatings Technology* 203, 3410–3419 (2009)
- [8]. Kalkancı, H.: Mikro Ark Oksidasyon Teknolojisi ve Alüminyum Alaşım Malzemelere Uygulanması. Sakarya University, Institute of Science and Technology ,Loadsek Thesis, 122s, Sakarya (2004)
- [9]. Li, Qingbiao., Jun Liang and Qing Wang: Plasma Electrolytic Oxidation Coatings on Lightweight Metals. *Modern Surface Engineering Treatments* (2013) (<http://dx.doi.org/10.5772/55688>).
- [10]. Malayoğlu U., Tekin C., Çakmak E.: Plazma Elektrolitik Oksitlenme Yöntemiyle Hafif Metallerin Kaplanması Mühendis ve Makine Volume:49 No:582, 3-9 (2008)
- [11]. Başoğlu, Y.: 2014. Mikro Ark Oksidasyon Yöntemi İle Kaplanmış AA6082 Alaşımının Farklı Yağlama Şartlarında Tribolojik Özelliklerinin İncelenmesi. Süleyman Demirel University, Institute of Science and Technology, Doctorate Thesis, 213s, Isparta (2011)
- [12]. Salman, Ö.: Yağlama Yağı İçin Bitkisel Yağların ve Esterlerinin Tribolojik Özelliklerinin İncelenmesi . Süleyman Demirel University, Institute of Science and Technology, Doctorate Thesis, 266s, Isparta (2011)
- [13]. Yurtseven, H.: Asansörlerde Kullanılan Fren Balatalarının Tribolojik Özelliklerinin Deneysel İncelenmesi. Süleyman Demirel University, Institute of Science and Technology, Master's Thesis, 58 pp, Isparta(2010)
- [14]. Yerokhin, A.L., Matthews, A., Dowey, S., Lyubimov, V.V.: *Treniei Iznos* 19, 5, 642, in Russian (1998)
- [15]. Nie, X., Leyland, A., Song, H.W., Yerokhin, A.L., Dowey, S.J., Matthews, A.: Thickness effects on the Mechanical Properties of Micro-Arc Discharge Oxide Coatings on Aluminum Alloys, *Surf. Coat. Tech.*, (116-119), 1055-1060 (1999)
- [16]. Krishna, L.R., Purnima, A.S., Sundararajan, G.: A Comparative Study of Tribological Behavior of Microarc Oxidation and Hard-Anodized Coatings, *Wear*, 261(10), 1095-1101 (2006)
- [17]. Polat, A.: 2017A, 6061 ve 7039 Alüminyum Alaşımlarının Mikro Ark Oksidasyon Yüzey Kaplama Yöntemi İle Sert Seramik Kaplanması. Koceli University Institute of Science and Technology, Doctoral Thesis, 260s, Kocaeli (2009)
- [18]. Wu, H., Zeng-Sun, J., Bei-Yu, L., Feng-Rong, Y., Xian-Yi, L., 2003. Characterization Of Microarc Oxidation Process On Aluminum Alloy. *Chinese Phys. Lett.*, 20 (10), 1815–1818.
- [19]. Venugopal, A., Panda, R., Manwatkar, S., Sreekumar, S., Krishna, L. R., Sundararajan, G.: Effect Of Micro Arc Oxidation Treatment On Localized Corrosion Behaviour Of AA7075 Aluminum Alloy in 3.5% NaCl Solution. *Trans. Nonferrous Met. Soc. China* 22, 700-710 (2012)
- [20]. Khan, R., H. U., Yerokhin, A., Li, L., Dong, H., Matthews, A.: Surface Characterization of DC Plasma Electrolytic Oxidation Treated 6082 Aluminum Alloy: Effect of Current Density and Electrolyte Concentration. *Surf. & Coat. Techn.*, 205, 1679-1688 (2010)
- [21]. Baydoğan, M., Kayalı, E. S.: Alüminyum Esaslı Endüstriyel Ürünlerin Yüzey Özelliklerinin Mikro Ark Oksidasyon İşlemiyle Geliştirilmesi. Tübitak project no: 107m038, 54s (2009)
- [22]. Stachowiak, G. W., Batchelor, A. W.: *Engineering Tribology*, Elsevier Amsterdam London New York Tokyo (1993)
- [23]. Zhou, F., Wang, Y., Ding, H., Wang, M., Yu, M., Dai, Z.: Friction Characteristic Of Micro-Arc Oxidative  $\text{Al}_2\text{O}_3$  Coatings Sliding Against Sin Balls In Various Environments. *Surface and Coating Technology*, 202, 3808-3814 (2008)
- [24]. Blanchett, T.A., Kennedy, F.E.: The Development of Transfer Films in Ultra-High Molecular Weight Polyethylene/Dtainless Steel Oscillatory Sliding .*Tribology Transactions*, Vol 32, pp. 371-379(1989)
- [25]. Kovaříková, I., Szewczyková, B., Blaškovič, P., Hodúlová, E., Lechovič, E.: Study and Characteristic of Abrasive Wear Mechanisms. (2009) [http://www.mtf.stuba.sk/docs/internetovy\\_casopis/2009/1/kovarikova.pdf](http://www.mtf.stuba.sk/docs/internetovy_casopis/2009/1/kovarikova.pdf)
- [26]. Malayoğlu, U., Tekin, K., C., Malayoğlu, U., Shrestha, S.: An Investigation into the Mechanical and Tribological Properties of Plasma Electrolytic Oxidation and Hard-Anodized Coatings on 6082 Aluminum Alloy. *Materials Science and Engineering, A* 528, 7451-7460 (2011)

Yusuf Başoğlu "Study Of Tribological Features Of AA6082 Material Coated With Micro Arc Oxidation (MAO) Method At Different Lubricating Conditions." American Journal of Engineering Research (AJER), vol. 7, no. 08, 2018, pp. 177-199